Journal of Nuclear Medicine, published on February 12, 2021 as doi:10.2967/jnumed.120.257279

Improved primary staging of marginal zone lymphoma by addition of CXCR4-directed PET/CT

Short running title: CXCR4 imaging in marginal zone lymphoma

Johannes Duell[1,2], Franziska Krummenast[1,2], Andreas Schirbel[2,3], Philipp Klassen[3], Samuel Samnick[2,3], Hilka Rauert-Wunderlich[2,4], Leo Rasche[1,2], Andreas K. Buck[2,3], Hans-Jürgen Wester[5], Andreas Rosenwald[2,4], Herrmann Einsele[1,2], Max S. Topp[1,2], Constantin Lapa[2,3,6], and Malte Kircher[2,3,6]

1. Department of Internal Medicine II, University Hospital Würzburg, Würzburg, Germany
2. Comprehensive Cancer Center (CCC) Mainfranken, Würzburg, Germany
3. Department of Nuclear Medicine, University Hospital Würzburg, Würzburg, Germany
4. Institute of Pathology, University of Würzburg, Würzburg, Germany
5. Pharmaceutical Radiochemistry, Technische Universität München, München, Germany
6. Nuclear Medicine, Medical Faculty, University of Augsburg, Augsburg, Germany

Disclaimer: HJW is the founder and shareholder of Scintomics, a company that entered into a joint venture with 1717 Life Science Ventures to establish PentixaPharm, the owner and distributor of the CXCR4-directed PET tracer Pentixafor. All other authors declare no conflicts of interest.

Corresponding author: Constantin Lapa, MD (constantin.lapa@uk-augsburg.de)
Nuclear Medicine
Medical Faculty
University of Augsburg
Stenglinstr. 2
86156 Augsburg, Germany
Telephone: (+49) 821-400-2050
Telefax: (+49) 821-400-3057

First author: Johannes Düll, MD (Duell_J@ukw.de)
Department of Internal Medicine II
University Hospital Würzburg
Oberdürrbacher Str. 6
97080 Würzburg, Germany

Word count: 5196

ABSTRACT

Positron emission tomography/computed tomography (PET/CT) with ^{18}F-fluorodesoxyglucose (FDG) is an integral component in the primary staging of most lymphomas. However, its utility is limited in marginal zone lymphoma (MZL) due to inconsistent FDG avidity. One diagnostic alternative could be the targeting of CXC-motif chemokine receptor 4 (CXCR4), shown to be expressed by MZL cells. This study investigated the value of adding CXCR4-directed ^{68}Ga-Pentixafor PET/CT (CXCR4 PET/CT) to conventional staging.

Methods

22 newly diagnosed MZL patients were staged conventionally and with CXCR4 PET/CT. Lesions exclusively identified by CXCR4 PET/CT were biopsied as standard of reference and compared to imaging results. The impact of CXCR4-directed imaging on staging results and treatment protocol was assessed.

Results

CXCR4 PET/CT correctly identified all patients with viable MZL and was superior to conventional staging ($P < 0.001$). CXCR4-directed imaging results were validated by confirmation of MZL in 16/18 PET-guided biopsy samples. Inclusion of CXCR4 PET/CT in primary staging significantly impacted staging results in almost half, and treatment protocols in one third of patients (upstaging, n = 7; downstaging, n = 3; treatment change, n = 8; $P < 0.03$).

Conclusions

CXCR4 PET/CT is a suitable tool in primary staging of MZL and holds the potential to improve existing diagnostic algorithms.

Key words: molecular imaging; primary diagnosis; CXCR4; PET; theranostics

INTRODUCTION

Marginal zone lymphomas (MZL) originate from malignantly transformed lymphocytes of the B-cell lineage and belong to the family of Non-Hodgkin Lymphomas. Three subtypes are differentiated according to their tissue of origin. The most common subtype is extranodal MZL (EMZL), which derives from mucosa-associated lymphoid tissue (MALT) and constitutes up to 70% of MZL cases. The splenic (SMZL) and nodal MZL subtypes (NMZL) are less common and affect primarily spleen or lymph nodes (LN), but can also be found in peripheral blood and/or bone marrow (BM) (*1*).

The therapeutic approach depends on results of staging according to the modified Ann Arbor system and includes BM biopsy, gastrointestinal endoscopy and computed tomography (CT). While limited disease (stages I and II) can often be irradiated with curative intent, either chemotherapy (± rituximab) is initiated or a watch & wait strategy is chosen in advanced stages. Positron emission tomography (PET)/CT with the radio-labeled glucose analog ^{18}F-fluorodesoxyglucose (FDG) is well-established and generally recommended as imaging modality of choice for initial evaluation and response assessment in all FDG-avid lymphomas (*2*). However, only 60 - 85% of MZL are FDG-avid, and while slightly superior to conventional CT imaging, FDG PET/CT tends to perform particularly poor in EMZL (*3,4*).

C-X-C motif chemokine receptor 4 (CXCR4) is widely expressed throughout the human body and plays a crucial role in embryonic development, homeostasis of the adult hematopoietic system, and modulation of the immune system (*5,6*). In addition, CXCR4 and its cognate ligand CXCL12 have shown to be of relevance in cancer growth and metastasis (*7,8*). CXCR4 is not only physiologically expressed on almost all lymphocytes,

but also observed on T and B cell neoplasms, including MZL (*9*). The expression of human CXCR4 can be non-invasively visualized *in vivo* by PET/CT imaging using radio-labeled receptor ligands like ^{68}Ga-Pentixafor, which has already demonstrated applicability in imaging a variety of (hemato-) oncologic and inflammatory diseases (*10-16*). Furthermore, first proof-of-concept studies with ^{68}Ga-Pentixafor PET (CXCR4 PET) have already demonstrated encouraging results in MZL patients (*17,18*).

In this analysis, we investigated the added value of including CXCR4 PET/CT in the primary staging algorithm of newly diagnosed, treatment-naïve MZL with respect to change of disease stage and impact on patient management. Conventional staging comprising BM biopsy, gastrointestinal endoscopy and FDG PET/CT served as standard of reference. To validate results of the new imaging approach, additional biopsies of exclusively CXCR4$^+$ lesions were obtained and evaluated for presence of MZL and CXCR4 expression.

MATERIALS AND METHODS

^{68}Ga-Pentixafor was administered in compliance with §37 of the Declaration of Helsinki, the German Medicinal Products Act, AMG §13 2b, and in accordance with the responsible regulatory body (Government of Upper Franconia; “Regierung von Oberfranken”, Germany). All patients underwent imaging for clinical purposes and gave written and informed consent to the diagnostic procedures. The local institutional review board (ethics committee of the University of Würzburg, Germany) approved this retrospective study (reference number 20201123 01).

Patients and Staging

Between May 2017 and January 2019, 22 consecutive patients (15 female, 7 male; mean age, 66 ± 9 years) were referred to our institution for further diagnostic work-up of newly diagnosed MZL of all subtypes (extranodal, *n* = 15; nodal, *n* = 6; splenic, *n* = 1). None of the patients had received treatment prior to imaging. Staging was done as recommended by the World Health Organization and the European Society for Medical Oncology using the modified Ann Arbor system (including FDG PET/CT, which is a local standard at our institution) (*19,20*), further complemented by CXCR4 PET/CT imaging within a median of 4 days of each other (range, 1 – 7 days). In addition to biopsies obtained during conventional staging (*n* = 85), tissue samples were taken from exclusively CXCR4$^+$ lesions (*n* = 18) if lymphoma detection implied a modification of the treatment protocol. Patient characteristics and information about CXCR4-guided biopsies are shown in Table 1.

In 12 cases follow-up imaging was available, depending on the respective tracer-avidity at primary staging with either one or both tracers (FDG, *n* = 5; CXCR4, *n* = 11).

PET/CT Imaging

^{68}Ga-Pentixafor and ^{18}F-FDG were synthesized in-house as previously described using a fully GMP compliant automated synthesizer (GRP, Scintomics, Fürstenfeldbruck, Germany) or a 16 MeV Cyclotron (GE PETtrace™ 6; GE Healthcare, Milwaukee, USA), respectively (*21*). CXCR4-directed and FDG PET/CT scans were performed on a dedicated PET/CT scanner (Siemens Biograph mCT 64; Siemens Medical Solutions, Erlangen, Germany), in case of FDG after a 6-hour fasting period to ensure serum glucose levels below 130 mg/dL, in case of ^{68}Ga-Pentixafor without any special patient preparation. Mean injected activity was 117 ± 27 MBq (range, 78 - 186 MBq) for ^{68}Ga-Pentixafor, and 298 ± 16 MBq (range, 263 - 334 MBq) for ^{18}F-FDG, respectively. There were no adverse or clinically detectable pharmacological effects in any of the 22 subjects. No significant changes in vital signs or the results of laboratory studies or electrocardiograms were observed. Whole-body (top of the skull to knees) PET scans were performed one hour after administration of the radiopharmaceutical. In CXCR4 PET, corresponding low-dose CT scans for attenuation correction and anatomical correlation were subsequently acquired (35 mAs, 120 keV, a 512 × 512 matrix, 5 mm slice thickness, increment of 30 mm/s, rotation time of 0.5 s, and pitch index of 0.8). In case of FDG PET a monophasic, contrast-enhanced CT (CARE Dose 4D, 160 mAs, 120 kV, 512 × 512 matrix, 5 mm slice thickness, slice collimation 64 × 0.6 mm, pitch index 1.4) was acquired. PET images were reconstructed using standard parameters (HD-PET, 3 iterations, 24 subsets, Gaussian filtering: 2 mm, resolution: axial resolution: 5 mm, in-plane resolution:

4 × 4 mm^2) with corrections for attenuation (CT-based), dead-time, random events and scatter.

Image Analysis

PET/CTs were separately analysed by two experienced investigators (CL and MK) blinded to the respective other PET scan as well as all other staging results. FDG uptake was rated according to the Lugano Classification (*22*). $CXCR4^+$ lesions were visually determined as focally increased tracer retention compared to surrounding normal tissue or contralateral structures. Images were first inspected visually. Then, the maximum standardized uptake value (SUV_{max}) of all potential lesions was derived by placing volumes of interest of at least 10 mm diameter around them. To normalize uptake and account for background activity, mean blood pool activity was measured by placing a 10 mm volume of interest in the right atrium. Then, a target-to-background ratio was calculated by dividing SUV_{max} (lesion) by SUV_{mean} (blood pool). Analysis of data was performed both on a per-patient and a per-lesion basis. For lesion analysis on a per-patient basis, subjects were categorized into one of four groups: (1) no detectable focal lesion (FL); (2) 1 to 5 FL; (3) 6 to 10 FL and (4) more than 10 FL. Furthermore, the lesion with the highest tracer uptake (hottest lesion) in the respective PET scans was used as a comparison parameter in the per-patient analysis.

Immunohistochemistry

In total, 103 biopsies were taken and examined for presence of MZL and for CXCR4 expression (gastrointestinal tract, *n* = 48; bone and BM, *n* = 24; lymph nodes and tonsils, *n* = 19; (salivary) glands, *n* = 3; other / soft tissues, *n* = 9). 17.5% (18/103) of these biopsies

were taken after the discovery of new lesions in CXCR4 PET, the remaining biopsies (85/103) were taken during conventional staging.

To confirm specific binding of ^{68}Ga-Pentixafor, paraffin sections (1 µm) derived from PET-guided biopsies were stained using an anti-CXCR4 rabbit polyclonal antibody (ab2074; Abcam, Cambridge, UK), and detected and visualized by using the Dako EnVision-HRP rabbit labeled polymer/DAB. Counterstaining was performed with hematoxylin. CXCR4 positivity of vascular epithelium served as internal and adrenocortical tissue as external positive control. Intensity of CXCR4 expression was visually rated using a 4-point scoring scale (0 = absent, 1 = weak, 2 = moderate, 3 = intense). To determine the proliferative activity of tumor cells, Ki-67 labeling index after immunostaining for MIB-1 (monoclonal, clone Ki-67, 1:50, Dako, Hamburg, Germany) was calculated by determining the number of positive nuclei under 100 lymphoma cells per high power field (x 400) in a total of 10 high power fields per sample. SUV_{mean} / SUV_{max} of the respective biopsied lesion was correlated to the intensity of receptor expression and proliferation activity.

Statistical analysis

All statistical testing was performed in SPSS Statistics 25 (IBM Corporation, Armonk, New York). The Kolmogorov-Smirnov test was used to verify a normal distribution of the data. Continuous parametric variables are expressed as mean ± 1 standard deviation. For group statistics, comparisons between MZL subtypes and GI-/BM-involvement were performed using one-way analysis of variance. Significance of the observed differences between groups was confirmed with a Games–Howell post-hoc test. Unpaired t-tests were used to compare uptake (ratios) of both tracers in corresponding lesions. Pearson's

correlation coefficients (r) were calculated to assess the association between uptake (ratios) of both tracers. *P* values ≤ 0.05 were considered statistically significant.

RESULTS

Considering all available information including follow-up, 20 patients had viable MZL manifestations at the time of imaging (EMZL, *n* = 14; NMZL, *n* = 5; SMZL, *n* = 1; true positive, TP), with 13.6% (3/22) of patients found to have BM infiltration and 18.2% (4/22) GI involvement, respectively. In two cases with limited disease stages, initial tissue sampling led to complete removal of all suspicious lesions (EMZL, *n* = 1; NMZL, *n* = 1; patients #1 and #6), and both patients remained in complete remissions without treatment during follow-up (true negative, TN). Staging results and its impact on treatment protocol are shown in Table 2.

Conventional Staging

Conventional staging based on FDG PET/CT, endoscopy and BM biopsy correctly identified 80.0% (16/20) of MZL patients (EMZL, 11/14; NMZL, 4/5; SMZL, 1/1), in the remaining 4 patients no lymphoma manifestations could be delineated (EMZL, 3/14; NMZL, 1/5). One of the two TN patients was correctly rated as negative, the other one as false positive (FP). All patients with gastrointestinal involvement (4/4), and 66.7% (2/3) of subjects with BM infiltration were identified. No lesions were found in 22.7% (n = 5), 1-5 lesions in 40.9% (n = 9), 6-10 lesions in 4.5% (n = 1), and >10 lesions in 31.8% (n = 7) of patients, respectively. Mean SUV_{max} (FDG) of the hottest lesion was 10.7 ± 9.9 (median 7.2; range, 2.3 – 39.6), while mean target-to-background ratio was 4.4 ± 5.8 (median 2.3; range, 0.8 – 25.6). Six subjects were classified as having limited disease (27.3%; Ann Arbor Stage I, *n* = 6; Stage II, *n* = 0) and 11 as having advanced disease (50.0%; Ann Arbor Stage III, *n* = 3; Stage IV, *n* = 8), respectively.

CXCR4 PET/CT

CXCR4 PET/CT correctly detected all TP (20/20) and TN (2/2) patients, as well as 75% (3/4) of patients with GI involvement and all (3/3) subjects with BM infiltration. No lesions were found in 9.1% (n = 2), 1-5 FL in 31.8% (n = 7), 6-10 FL in 13.6% (n = 3) and >10 FL in 45.5% (n = 10) of patients, respectively. Mean SUV_{max} (CXCR4) of the hottest lesion was 13.0 ± 6.4 (median 11.7; range, 3.7 – 27.4), while mean target-to-background ratio was 4.8 ± 2.5 (median 4.0; range, 2.1 – 10.7). Based on CXCR4-directed imaging, 36.4% of patients were classified as having limited stage disease (n = 8; Ann Arbor Stage I, *n* = 3; Stage II, *n* = 5), 54.5% of patients as suffering from an advanced disease stage (n = 12; Ann Arbor Stage III, *n* = 2; Stage IV, *n* = 10), respectively.

Biopsy results

Overall, 31.1% of tissue samples confirmed the presence of MZL (32/103; GI tract, *n* = 7; bone/BM, *n* = 5; lymph nodes/tonsils, *n* = 11; (salivary) glands, *n* = 3; other/soft tissue, *n* = 6).

Of the biopsies taken during conventional staging 18.8% (16/85) confirmed MZL, with evidence of GI involvement in 10.9% (5/46) of specimens (patients #4, #11, #12 and #19) and of BM infiltration in 9.1% (2/22) of biopsies taken (patients #16 and #17), respectively.

88.9% (16/18) of samples taken from exclusively $CXCR4^+$ lesions confirmed MZL. Details of biopsy locations and results are shown in Table 1 (also, maximum intensity projection images [MIPs] of all PET scans with biopsy locations are provided in the Supplemental File as Supplemental Figures 1 - 22).

Comparison of conventional staging and CXCR4 PET

The difference in detection of MZL between CXCR4 PET/CT and conventional staging was significant, with correct detection of all viable MZL and TN cases by CXCR4 PET/CT, while conventional staging only identified 16/20 TP and 1/2 TN subjects, respectively (22/22 vs. 17/22; $P < 0.001$).

Regarding GI involvement, CXCR4 PET/CT was not inferior to regular staging (4/4 vs. 3/4; $P = n.s.$). Similarly, there was no significant difference in detection of BM infiltration (3/3 vs. 2/3; $P = n.s.$). Of note, in one case BM infiltration was only identified due to CXCR4-guided biopsy whereas the random iliac crest biopsy taken during conventional staging was (false) negative. Examples of exclusively $CXCR4^+$ lesions in EMZL and gastric MZL are given in Figures 1 and 2.

No significant difference between the two tracers was found when comparing the respective hottest lesions (^{18}F-FDG, 10.7 ± 9.9 vs. ^{68}Ga-Pentixafor, 13.0 ± 6.4; $P = 0.36$). Similarly, target-to-background ratios of FDG and CXCR4 PET did not show significant differences (4.4 ± 5.8 vs. 4.8 ± 2.5; $P = 0.90$).

Results from CXCR4 PET/CT led to up-/downstaging and change of treatment in a significant number of patients (total, 10/22; upstaging, $n = 7$; downstaging, $n = 3$; treatment change, $n = 8$; $P < 0.03$). The effects on patient management included both escalation (27.3%, $n = 6$) and de-escalation (9.1%, $n = 2$) of therapy (Table 2).

Immunohistochemistry

Staining for CXCR4 in confirmed specimens of MZL showed a highly variable receptor expression on the surface of MZL cells with receptor expression intensities ranging from 0 - 2. Various of the confirmed MZL lesions identified by CXCR4 PET/CT showed relatively

low receptor expression on the cell surface with a “dot-like” pattern. An intense staining of the residual germinal center B-cells occurred particularly in nodal MZL manifestations (Figure 3). Ki-67 index ranged from 5% to 40% (mean, 14.4 ± 7.7), and correlated positively with uptake of both tracers (SUV_{mean} and SUV_{max}: ^{68}Ga-Pentixafor, r = 0.56, $P < 0.05$; FDG, r = 0.71, $P < 0.01$; respectively). Intensity of immunohistopathological staining was not significantly related with CXCR4-directed PET uptake (SUV_{mean}, r = -0.20; SUV_{max}, r = -0.21, P = n.s.).

DISCUSSION

This pilot study in a homogeneous cohort of patients with newly diagnosed, treatment-naïve lymphoma clearly demonstrates the ability of CXCR4 PET/CT for primary staging of MZL with all patients with viable MZL being correctly identified. Whereas a recent study from Austria utilizing CXCR4-directed PET/MRI also reported on the general feasibility of CXCR4 PET for visualizing MALT lymphoma (*18*), this is the first study to provide a systematic comparison to conventional staging including bone marrow biopsy, endoscopy and FDG PET/CT and to assess the impact of CXCR4-directed imaging on patient management in all subjects.

Compared to conventional staging, CXCR4 PET/CT detected significantly more MZL manifestations, both on a per-patient as well as on a per-lesion basis ($P < 0.001$). Noteworthy, lesions exclusively unveiled by the new imaging approach could be confirmed in locations easily missed in conventional (PET/)CT imaging such as subcutaneous tissue or orbital masses. In addition, our data also indicate non-inferiority of CXCR4 PET/CT in detection of GI tract lesions and BM infiltration (as compared to endoscopy and bone marrow biopsy, respectively) – sites that also pose a diagnostic challenge to imaging.

The results of imaging and biopsies are consistent with the existing literature showing robust CXCR4 expression of MZL cells in more than 90% of cases (*9,23*). Furthermore, prior studies have reported relatively heterogeneous FDG-avidity of MZL, concordant to our data with many of the biopsy-proven, FDG-negative lymphoma manifestations (*3,4*). Also noteworthy is a recent study in patients with lymphoplasmacytic lymphoma that reported similar findings to ours, showing superior lymphoma detection by CXCR4 PET/CT in comparison to FDG PET/CT (*16*).

Thus, CXCR4-directed imaging might prove a suitable new imaging tool for comprehensive whole-body staging of MZL as well as other non FDG-avid lymphoma types as it might enable a more accurate detection of lymphoma lesions and consequently better stage-adjusted treatment strategies.

With regards to patient management, one of the main findings of our study is that the improved detection rate of CXCR4 PET/CT had a significant impact on staging according to the modified Ann Arbor classification system, as information exclusively gained by CXCR4 PET/CT led to a re-classification in almost half of patients with the majority of subjects being up-staged. This in turn had a direct effect on patient management, as more than one third of patients (8/22, 36.4%) had their treatment protocol modified due to the new information; most often local treatment approaches were abandoned for the sake of systemic chemotherapy or watch-and-wait strategies due to the visualization of previously occult MZL manifestations. In an approach to provide a robust standard of reference for lesions with discrepant PET imaging results, biopsies were stringently obtained. Underlining the improved sensitivity of CXCR4-directed imaging, 88.9% (16/18) of the biopsies from $CXCR4^{+}$ lesions were true positives, compared to only 18.8% (16/85) true positive biopsies obtained during conventional staging. Interestingly, very few false positive lesions (2/18; 11.1%) were encountered, which is remarkable considering the large number of other cell types expressing CXCR4 on their cell surface, including inflammatory B and T cells, macrophages and neutrophils (*6*). Therefore, it cannot be ruled out that at least part of the PET signal originates from additional, yet unknown, non-lymphoma cell types.

It is worth mentioning that the proliferation activity (as indicated by Ki-67 index) of MZL lesions correlated positively with the intensity of the respective PET imaging signal.

While the association between tumor aggressiveness and ^{18}F-FDG uptake is well established, our findings underscore an additional potential prognostic value of CXCR4 PET in MZL and is in line with results of previous pathology studies (*9*).

The utility of CXCR4 PET/CT in re-staging has not yet been demonstrated. While first data in a subject with EMZL of the orbital cavities (*17*) suggest that the new technique holds potential for the non-invasive assessment of therapy response and patient follow-up (especially in cases with ambiguous findings in conventional imaging), the added value of CXCR4-directed PET imaging in this setting also needs to be investigated.

Given the physiologically high splenic tracer uptake/retention in CXCR4 PET/CT, splenic marginal zone lymphoma is likely to pose a diagnostic challenge to this new imaging approach.

Limitations

Our study has various limitations including its retrospective nature and the small sample size, thus limiting statistical power. Furthermore, although histology could prove presence of MZL and CXCR4 expression on cells in most of the biopsy specimens, receptor expression was relatively heterogeneous and did not perfectly correlate with PET imaging findings. However, histology results might be influenced by biopsy yields and by receptor kinetics and internalization, given that CXCR4 expression at the cell surface is dynamically regulated and receptor internalization is induced by ligand binding. In contrast, strengths of our study include the stringent acquisition of histological evidence that the PET signal originates from CXCR4 positive MZL cells, as determined by immunohistochemical work-up of tissue samples obtained from PET-guided biopsies. In addition, all patients were

newly diagnosed, treatment-naïve and underwent the full recommended diagnostic work-up (including FDG PET/CT).

CONCLUSION

In summary, our data shows that primary staging of MZL using CXCR4 PET/CT is feasible and has significant impact on staging results and treatment choice.

Although present data suggest that CXCR4 PET/CT has the potential to be the new imaging standard in MZL, various questions are still to be answered until its use can be unanimously recommended: Whether CXCR4 PET/CT will have an impact on progression-free-survival, overall survival, quality of life or healthcare costs has to be determined in larger, prospective studies.

Key Points

QUESTION: What impact does inclusion of CXCR4-directed PET/CT imaging into the primary staging algorithm of marginal zone lymphoma have on staging results and treatment choice?

PERTINENT FINDINGS: This is the first study to provide a systematic comparison between conventional staging including bone marrow biopsy, endoscopy and FDG PET/CT and CXCR4-directed imaging in MZL.

CXCR4 PET/CT detected significantly more MZL manifestations and had a significant impact on Ann Arbor staging with a re-classification in almost half of patients and eventually patient management in more than one third of cases.

IMPLICATIONS FOR PATIENT CARE: Our data suggest that CXCR4 PET/CT has the potential to be the new imaging standard.

REFERENCES

1. Swerdlow S, Campo E, Harris N, et al. WHO classification of tumours, revised 4th edition. 2017:223-265.

2. Barrington SF, Kluge R. FDG PET for therapy monitoring in Hodgkin and non-Hodgkin lymphomas. *Eur J Nucl Med Mol Imaging.* 2017;44:97-110.

3. Hoffmann M, Kletter K, Becherer A, Jäger U, Chott A, Raderer M. 18F-fluorodeoxyglucose positron emission tomography (18F-FDG-PET) for staging and follow-up of marginal zone B-cell lymphoma. *Oncology.* 2003;64:336-340.

4. Treglia G, Zucca E, Sadeghi R, Cavalli F, Giovanella L, Ceriani L. Detection rate of fluorine-18-fluorodeoxyglucose positron emission tomography in patients with marginal zone lymphoma of MALT type: a meta-analysis. *Hematol Oncol.* 2015;33:113-124.

5. Griffith JW, Sokol CL, Luster AD. Chemokines and chemokine receptors: Positioning cells for host defense and immunity. *Annu Rev Immunol.* 2014;32:659-702.

6. Hughes CE, Nibbs RJB. A guide to chemokines and their receptors. *Febs j.* 2018;285:2944-2971.

7. Müller A, Homey B, Soto H, et al. Involvement of chemokine receptors in breast cancer metastasis. *Nature.* 2001;410:50-56.

8. Zlotnik A, Burkhardt AM, Homey B. Homeostatic chemokine receptors and organ-specific metastasis. *Nat Rev Immunol.* 2011;11:597-606.

9. Stollberg S, Kämmerer D, Neubauer E, et al. Differential somatostatin and CXCR4 chemokine receptor expression in MALT-type lymphoma of gastric and extragastric origin. *J Cancer Res Clin Oncol.* 2016;142:2239-2247.

10. Wester HJ, Keller U, Schottelius M, et al. Disclosing the CXCR4 expression in lymphoproliferative diseases by targeted molecular imaging. *Theranostics.* 2015;5:618-630.

11. Lapa C, Schreder M, Schirbel A, et al. [(68)Ga]Pentixafor-PET/CT for imaging of chemokine receptor CXCR4 expression in multiple myeloma - Comparison to [(18)F]FDG and laboratory values. *Theranostics.* 2017;7:205-212.

12. Philipp-Abbrederis K, Herrmann K, Knop S, et al. In vivo molecular imaging of chemokine receptor CXCR4 expression in patients with advanced multiple myeloma. *EMBO Mol Med.* 2015;7:477-487.

13. Kircher M, Herhaus P, Schottelius M, et al. CXCR4-directed theranostics in oncology and inflammation. *Ann Nucl Med.* 2018;32:503-511.

14. Lapa C, Lückerath K, Kleinlein I, et al. (68)Ga-Pentixafor-PET/CT for imaging of chemokine receptor 4 expression in glioblastoma. *Theranostics.* 2016;6:428-434.

15. Kircher M, Tran-Gia J, Kemmer L, et al. Imaging inflammation in atherosclerosis with CXCR4-directed (68)Ga-Pentixafor PET/CT: Correlation with (18)F-FDG PET/CT. *J Nucl Med.* 2020;61:751-756.

16. Luo Y, Cao X, Pan Q, Li J, Feng J, Li F. (68)Ga-Pentixafor PET/CT for imaging of chemokine receptor 4 expression in Waldenström Macroglobulinemia/Lymphoplasmacytic Lymphoma: Comparison to (18)F-FDG PET/CT. *J Nucl Med.* 2019;60:1724-1729.

17. Herhaus P, Habringer S, Vag T, et al. Response assessment with the CXCR4-directed positron emission tomography tracer [(68)Ga]Pentixafor in a patient with extranodal marginal zone lymphoma of the orbital cavities. *EJNMMI Res.* 2017;7:51.

18. Haug AR, Leisser A, Wadsak W, et al. Prospective non-invasive evaluation of CXCR4 expression for the diagnosis of MALT lymphoma using [(68)Ga]Ga-Pentixafor-PET/MRI. *Theranostics.* 2019;9:3653-3658.

19. Lister TA, Crowther D, Sutcliffe SB, et al. Report of a committee convened to discuss the evaluation and staging of patients with Hodgkin's disease: Cotswolds meeting. *J Clin Oncol.* 1989;7:1630-1636.

20. Zucca E, Arcaini L, Buske C, et al. Marginal zone lymphomas: ESMO Clinical Practice Guidelines for diagnosis, treatment and follow-up. *Ann Oncol.* 2020;31:17-29.

21. Martin R, Juttler S, Muller M, Wester HJ. Cationic eluate pretreatment for automated synthesis of [(6)(8)Ga]CPCR4.2. *Nucl Med Biol.* 2014;41:84-89.

22. Cheson BD, Fisher RI, Barrington SF, et al. Recommendations for initial evaluation, staging, and response assessment of Hodgkin and non-Hodgkin lymphoma: the Lugano classification. *J Clin Oncol.* 2014;32:3059-3068.

23. Trentin L, Cabrelle A, Facco M, et al. Homeostatic chemokines drive migration of malignant B cells in patients with non-Hodgkin lymphomas. *Blood.* 2004;104:502-508.

Figures

Figure 1: Example of Extranodal Marginal Zone Lymphoma (EMZL).

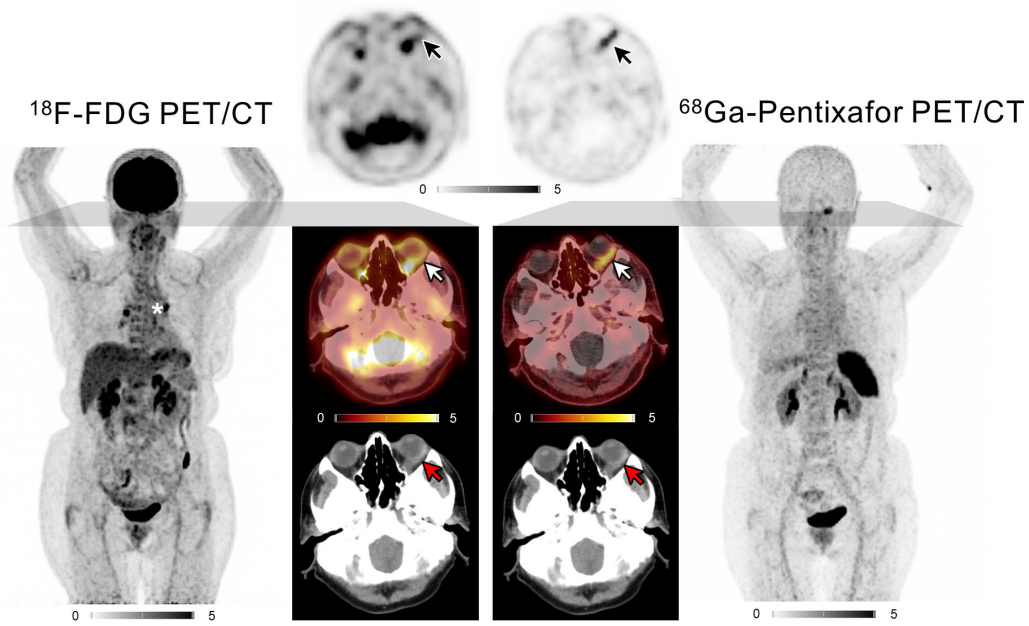

Patient #5 suffering from Extranodal Marginal Zone Lymphoma (EMZL) with Maximum Intensity Projections (MIPs) of FDG (left side) and ^{68}Ga-Pentixafor (right side) PET scans. In the center of the image, axial PET (top), PET/CT (middle) and CT (bottom) sections of a lymphoma manifestation in the left orbita with discrepant tracer uptake (FDG negative, CXCR4 positive) are shown as indicated by the white (PET/CT fusion images), black (PET only images) and red arrows (CT only). Of note: The white star indicates intense focal uptake of two hilar lymph nodes (FDG PET/CT); biopsy results revealed sarcoidosis, not MZL.

Figure 2: Example of Gastric Marginal Zone Lymphoma.

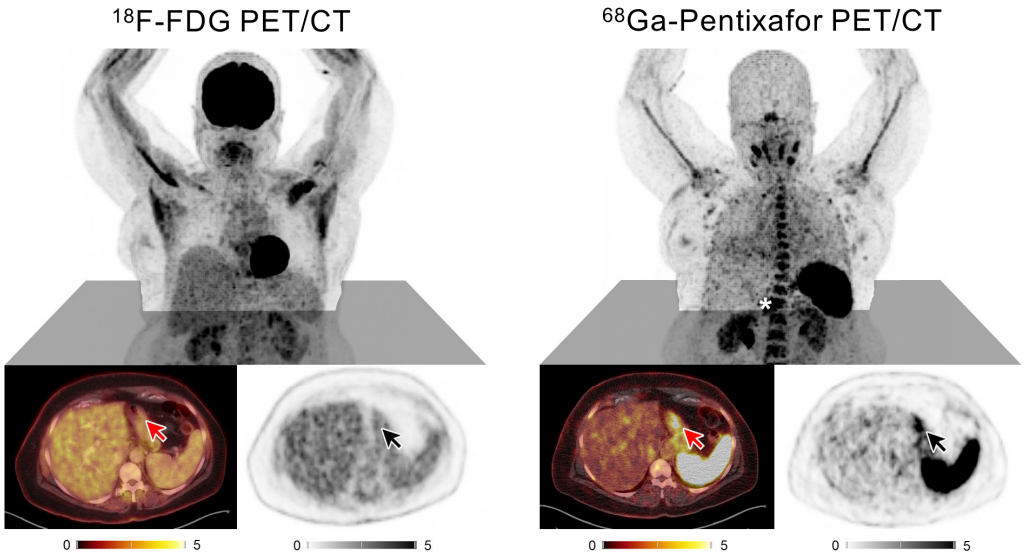

Patient #11 suffering from gastric Marginal Zone Lymphoma (MZL) with Maximum Intensity Projections (MIPs) of FDG (left side) and ^{68}Ga-Pentixafor (right side) PET scans. The lower part of the image shows axial sections of gastric lymphoma manifestations with discrepant tracer uptake (FDG negative, CXCR4 positive) as indicated by the white (PET/CT fusion images) and black arrows (PET only images). The white star indicates the gastric lymphoma in the ^{68}Ga-Pentixafor MIP image.

Figure 3: Immunohistochemistry and corresponding PET/(CT) scans of a MZL lesion in the right parotid gland.

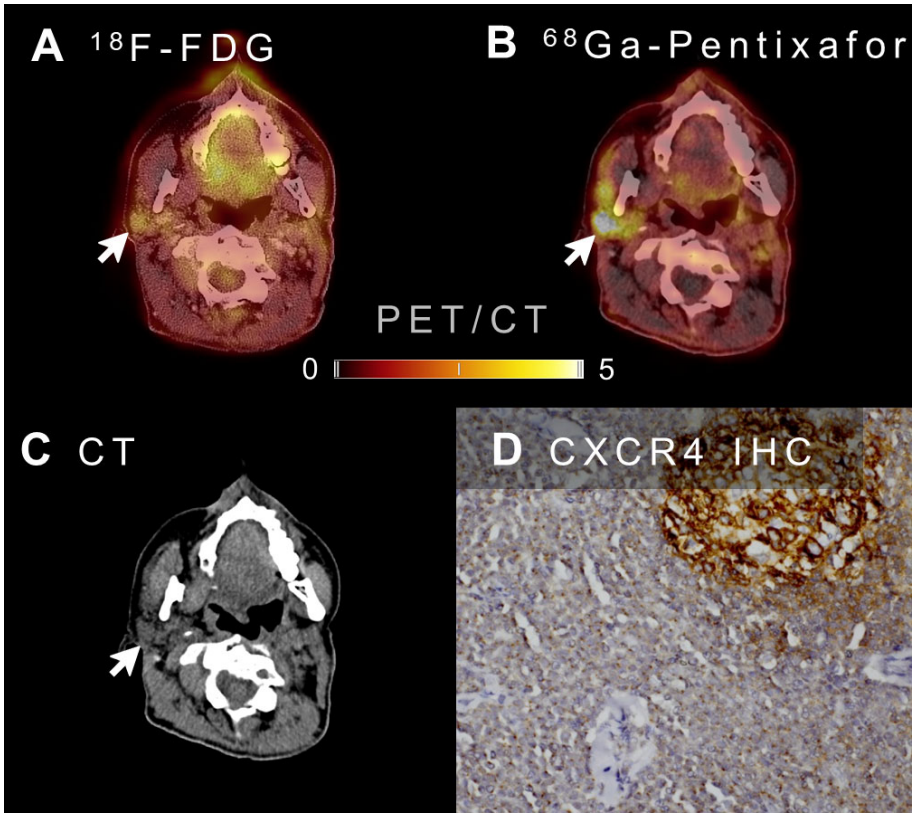

Data of patient #20: Hybrid FDG and CXCR4 PET/CT (A, B) CT only images (C) as well as Immunohistochemistry (IHC) of biopsy material from Marginal Zone Lymphoma of the parotid gland (D). The white arrows indicate discrepant tracer uptake (FDG negative, CXCR4 positive) in the respective fusion images. IHC for CXCR4 is showing strong staining in residual germinal center B-cells and distinct, often dot-like staining in the neoplastic marginal zone B-cell infiltrate.

Tables

Table 1: Patient characteristics and locations of CXCR4-guided biopsies

#	Sex	Age	MZL subtype	Location/Source of primary histology	Location of CXCR4-guided biopsy	Confirmation of MZL ?
1	M	51	EMZL/MALT	Lung	N/A	N/A
2	M	50	EMZL/MALT	Lung, multifocal	Lung	yes
3	F	70	NMZL	LN, axilla	LN, axilla	yes
4	F	56	EMZL/MALT	Salivary gland, sublingual	Salivary gland, lower lip	yes
5	F	76	EMZL/MALT	Orbita (no confirmation of MZL)	Orbita	yes
6	F	69	NMZL	LN, inguinal	N/A	N/A
7	F	79	EMZL/MALT	Cutaneous	Subcutaneous, thigh	yes
8	F	63	EMZL/MALT	Lacrimal gland	Conjunctiva + LN, axilla	no (conjunctiva), yes (LN)
9	F	70	NMZL	LN, cervical (right)	LN, cervical (left)	yes
10	F	66	NMZL	LN, cervical	LN, cervical	yes
11	F	62	EMZL/MALT	LN, cervical (negative)	Stomach	yes
12	M	68	EMZL/MALT	N/A	Ileum	yes
13	M	57	EMZL/MALT	LN, cervical	LN, axilla	no (not enough material)
14	M	80	EMZL/MALT	Orbita (right)	Orbita (left)	yes
15	F	57	EMZL/MALT	Bulk, mesenterial	LN, cervical	yes
16	F	63	NMZL	LN, axilla	LN, axilla + BM biopsy	yes (both)
17	F	72	SMZL	Splenectomy	LN, axilla	yes
18	F	71	EMZL/MALT	N/A	Bone, tibia	yes
19	M	69	EMZL/MALT	Stomach	Tonsil, Tonsils	yes (all three)
20	F	52	EMZL/MALT	LN, cervical (right)	Parotid gland	yes
21	M	72	NMZL	LN, retroperitoneal	Soft tissue formation perirenal	yes
22	F	59	EMZL/MALT	N/A	Parotid gland	yes

EMZL indicates extranodal marginal zone lymphoma; F, female; LN, lymph node; M, male; MALT, mucosa-associated lymphoid tissue; MZL, marginal zone lymphoma; NMZL, nodal marginal zone lymphoma; and SMZL, splenic marginal zone lymphoma.

Table 2: Staging results and impact on patient management

	Rated positive for MZL		BM / GI involvement		Ann Arbor Classification		Changes due to CXCR4 PET/CT	
#	Conv.	CXCR4	Conv.	CXCR 4	Conv.	CXCR4	Staging	Treatment protocol (initially planned)
1	yes*	no			I	-	Down	de-escalation to watch & wait (RTx)
2	yes	yes		BM	IV	IV		
3	yes	yes			IV	IV		
4	yes	yes	GI		I	IV	Up	
5	no	yes			-	I	Up	escalation to RTx (none)
6	no	no			-	-		
7	yes	yes			IV	IV		escalation to CTx (RTx); at f/u: CXCR4⁺ lesion → RTx
8	yes	yes			I	IV	Up	escalation to RTx of 3 lesions (RTx 1 lesion)
9	no	yes			-	II	Up	escalation to RTx (none)
10	yes	yes			III	III		
11	yes	yes	GI	GI, BM*	I	IV	Up	escalation of RTx (smaller radiation field)
12	yes	yes	GI	GI	I	I		
13	yes	yes			III	II	Down	
14	yes	yes			IV	II	Down	
15	yes	yes	BM*	BM*	IV	IV		
16	yes	yes	BM	BM	IV	IV		
17	yes	yes	BM	BM	IV	IV		
18	yes	yes			I	I		
19	yes	yes	GI	GI	IV	IV		de-escalation to watch & wait (RTx)
20	no	yes			-	II	Up	escalation to RTx (none)
21	yes	yes			III	III		
22	no	yes	GI*		-	II	Up	

* false-positive; BM indicates bone marrow; GI, gastrointestinal; Conv, conventional staging; CTx, chemotherapy; f/u, follow-up; MZL, marginal zone lymphoma; and RTx, radiation. Parentheses in the last column indicate initially planned therapy.

Graphical Abstract

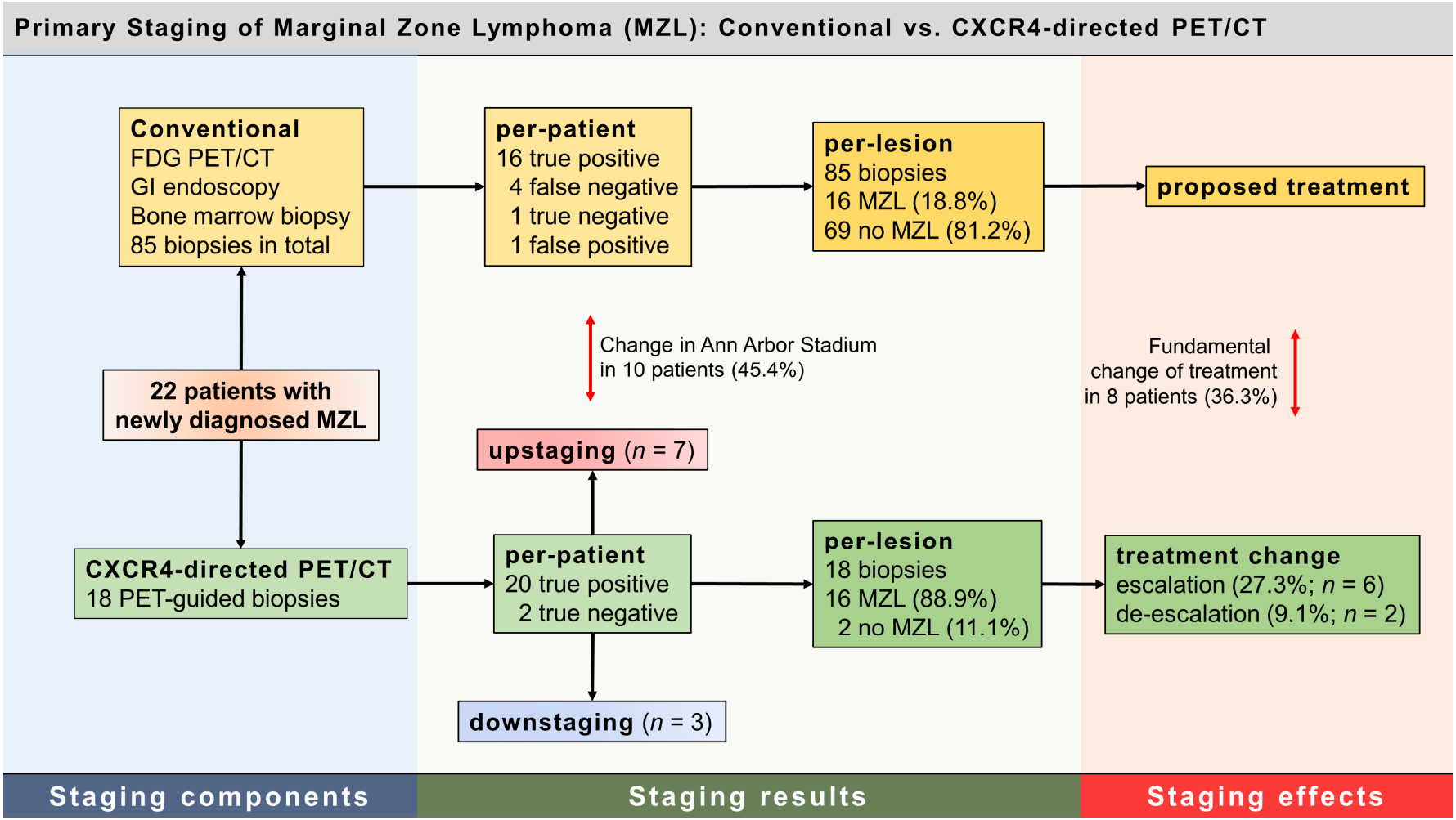

Supplemental File

Maximum Intensity Projections (MIPs) of all PET scans with location of (PET-guided) biopsies (Supplemental Figures 1 - 22).

CXCR4 PET/CT-guided biopsy with confirmation of MZL

CXCR4 PET/CT-guided biopsy without confirmation of MZL

FDG PET/CT-guided biopsy

Supplemental Figure 1: MIPs of FDG/CXCR4 PETs of patient #1

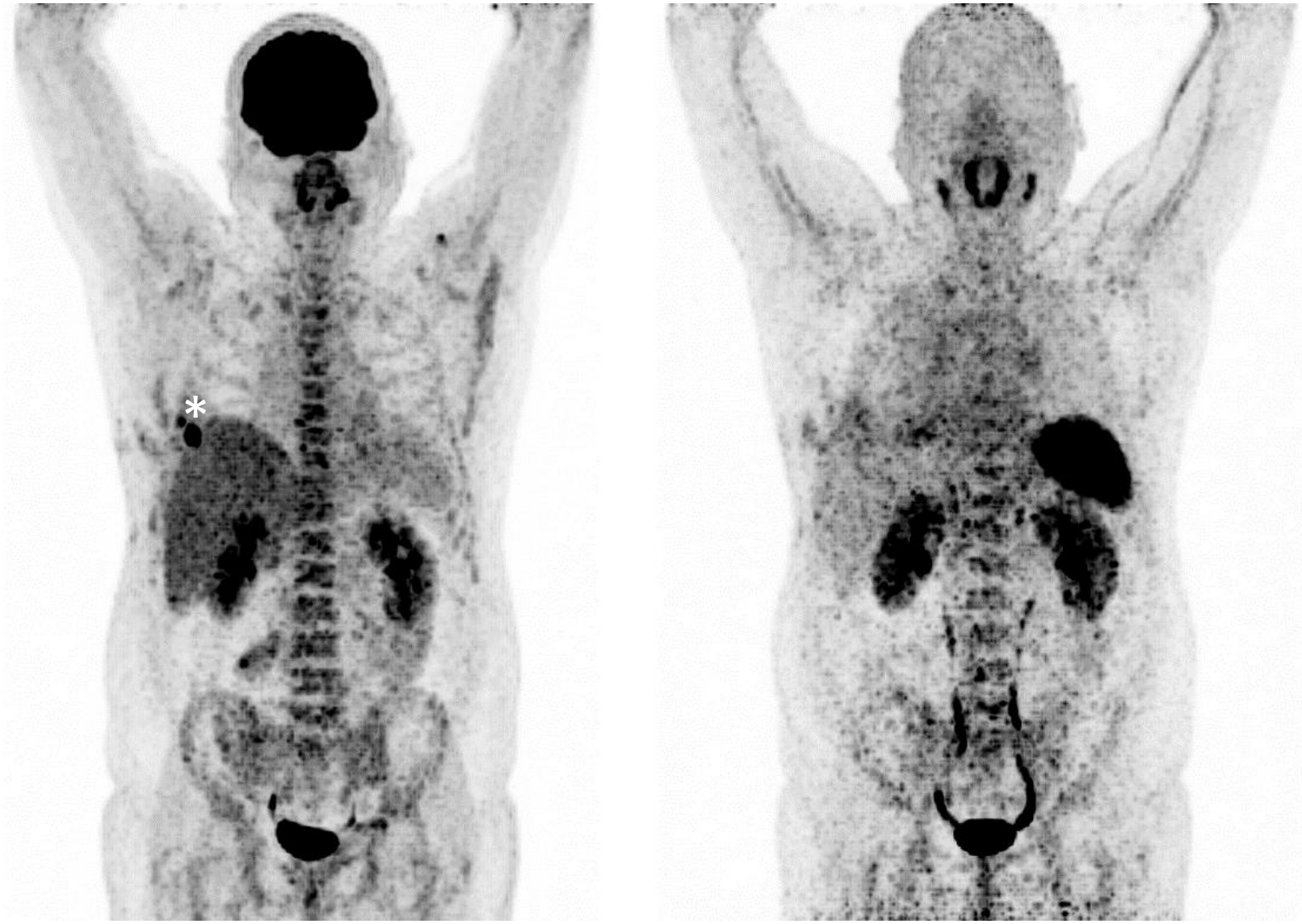

* The focal FDG-uptake was traceable to fractured ribs after resection of pulmonary lymphoma

Supplemental Figure 2: MIPs of FDG/CXCR4 PETs of patient #2

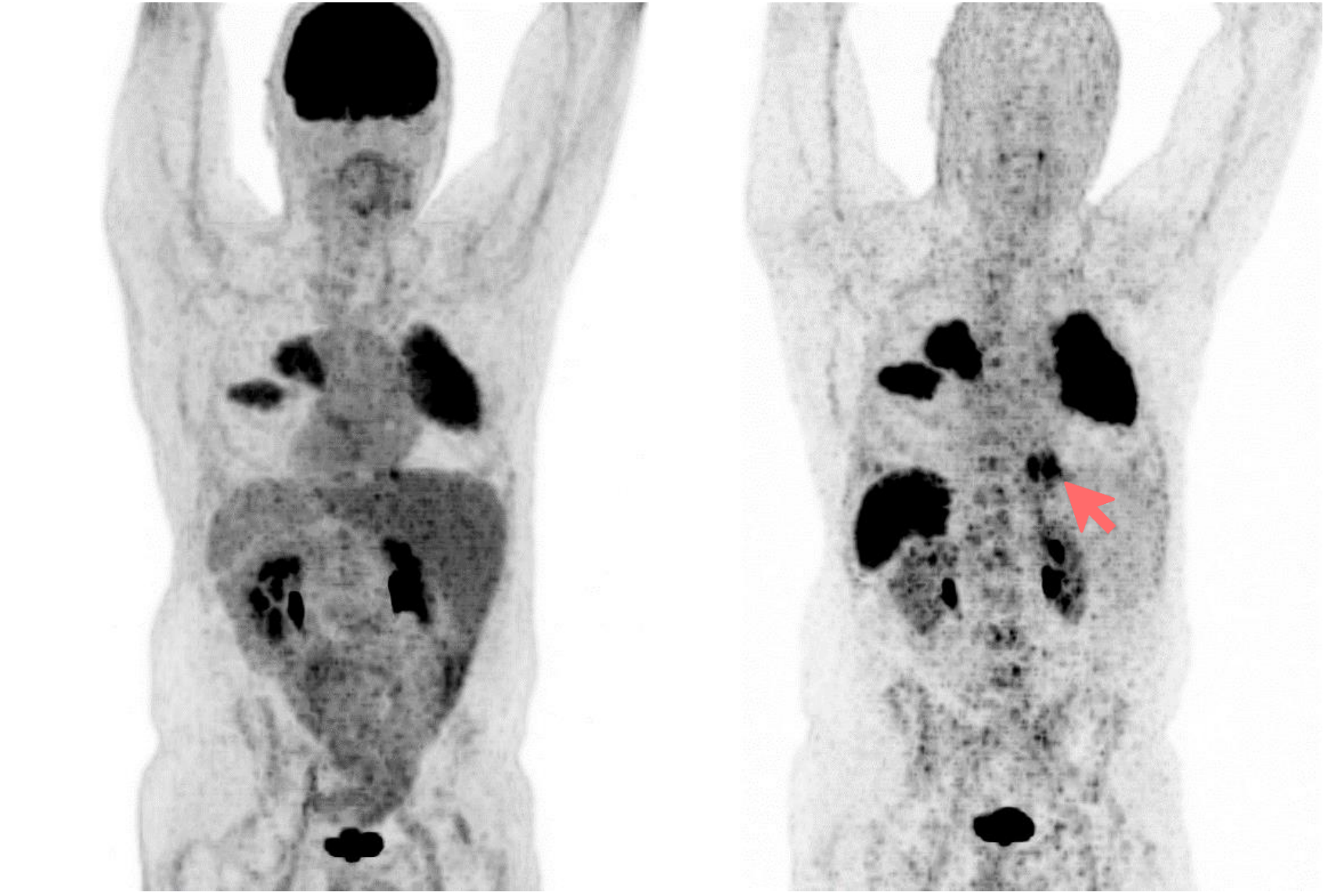

Supplemental Figure 3: MIPs of FDG/CXCR4 PETs of patient #3

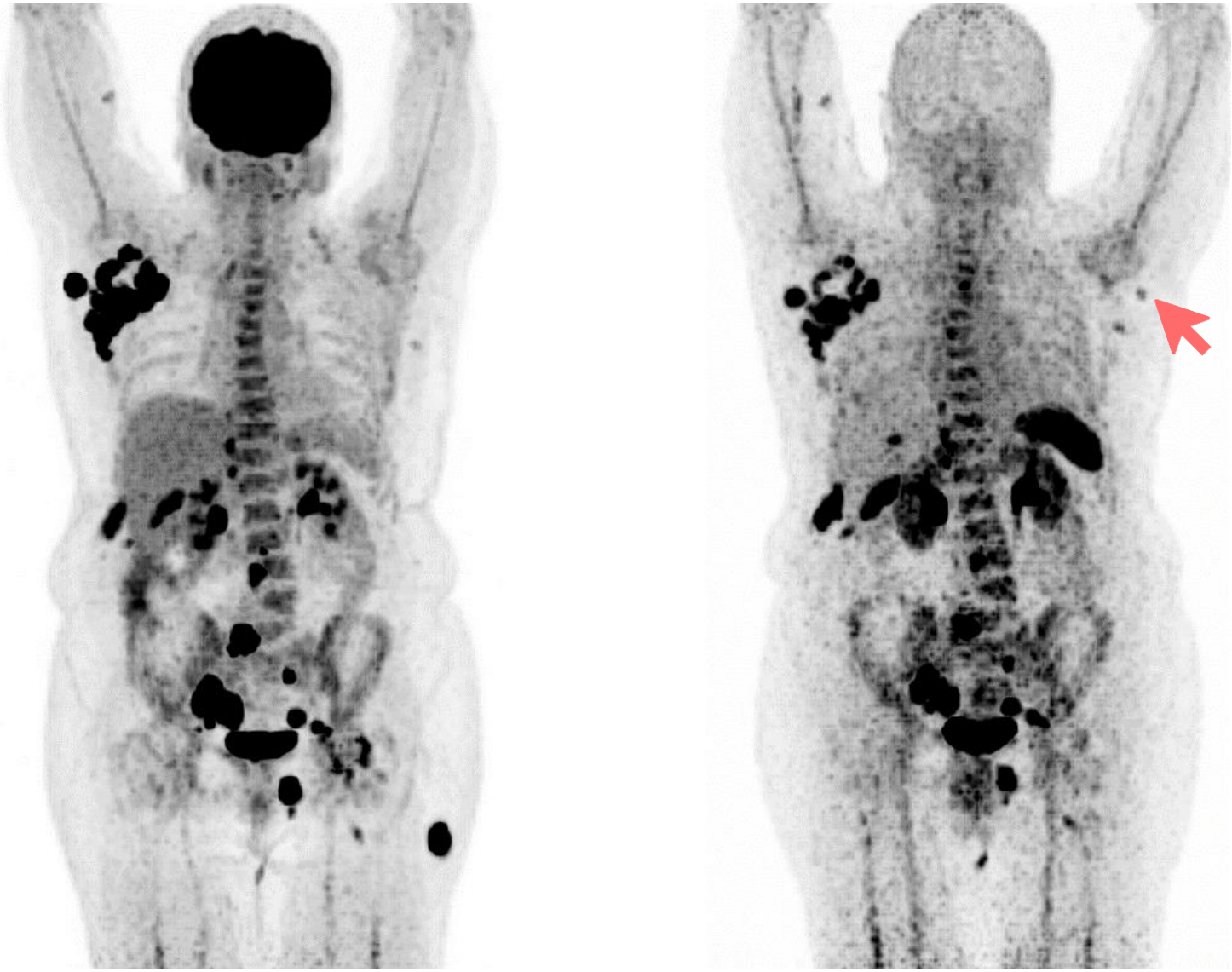

0 5

FDG CXCR4

Supplemental Figure 4: MIPs of FDG/CXCR4 PETs of patient #4

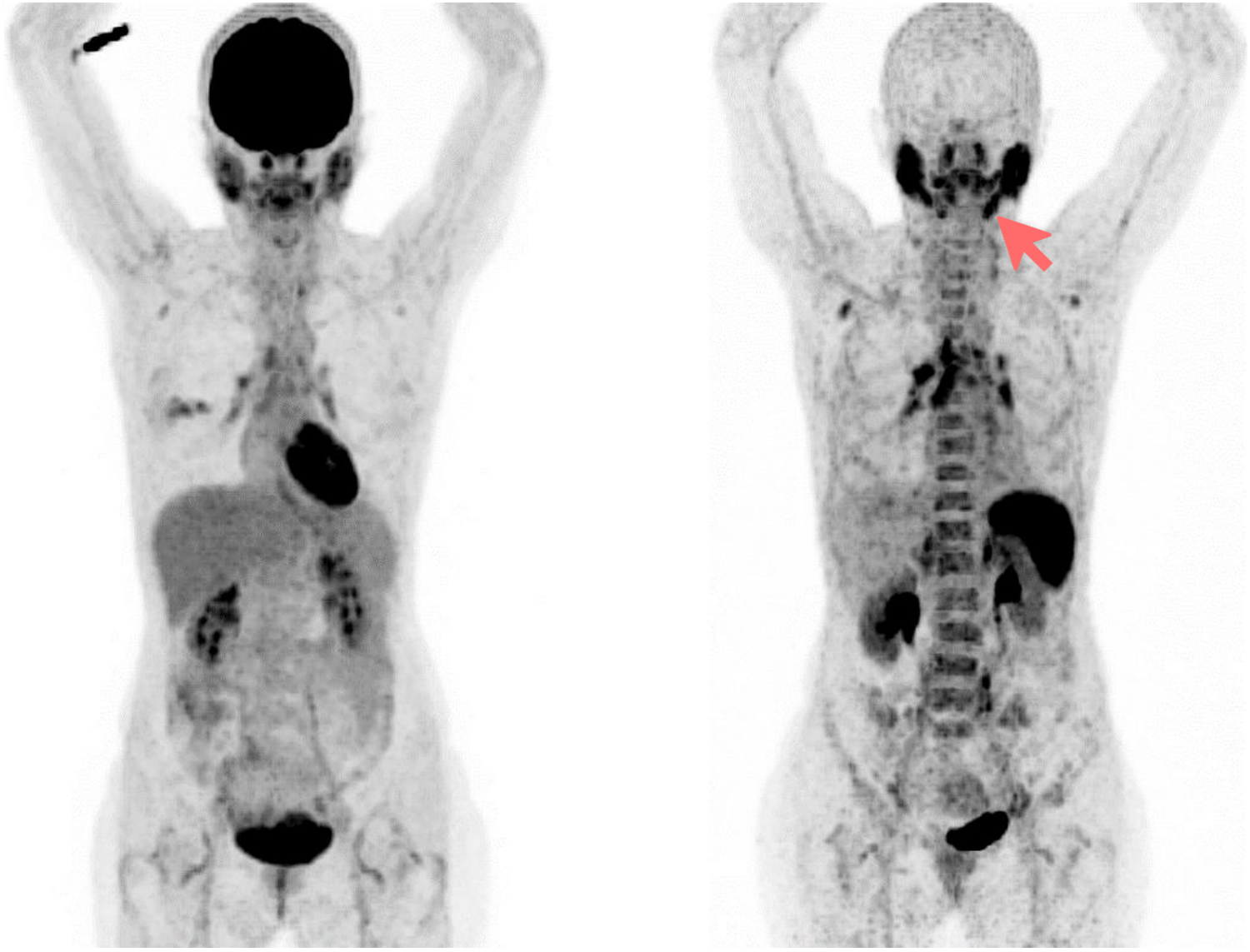

Supplemental Figure 5: MIPs of FDG/CXCR4 PETs of patient #5

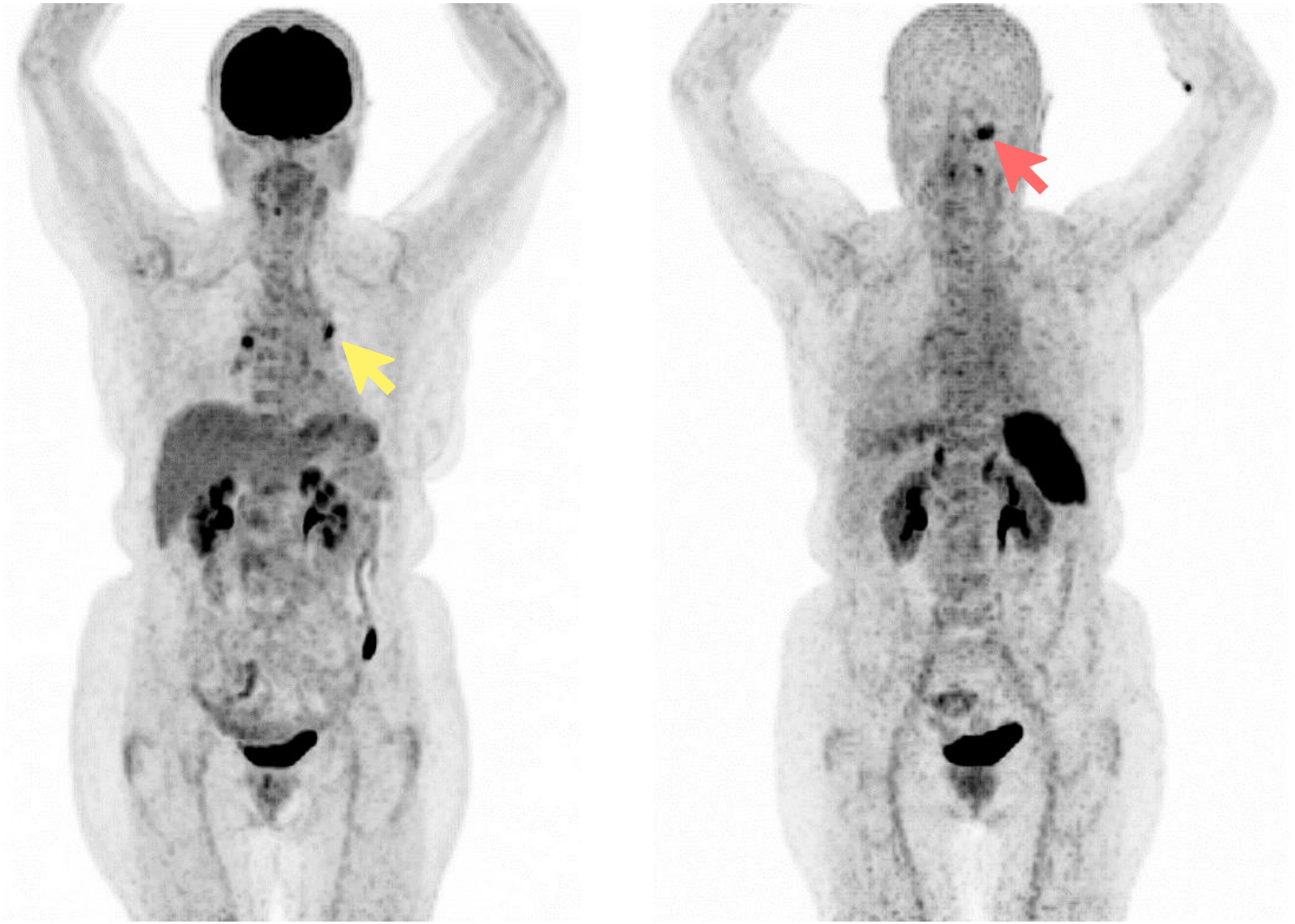

Yellow arrow: Biopsy of bihilar lymph nodes revealed sarcoidosis, but not lymphoma

Supplemental Figure 6: MIPs of FDG/CXCR4 PETs of patient #6

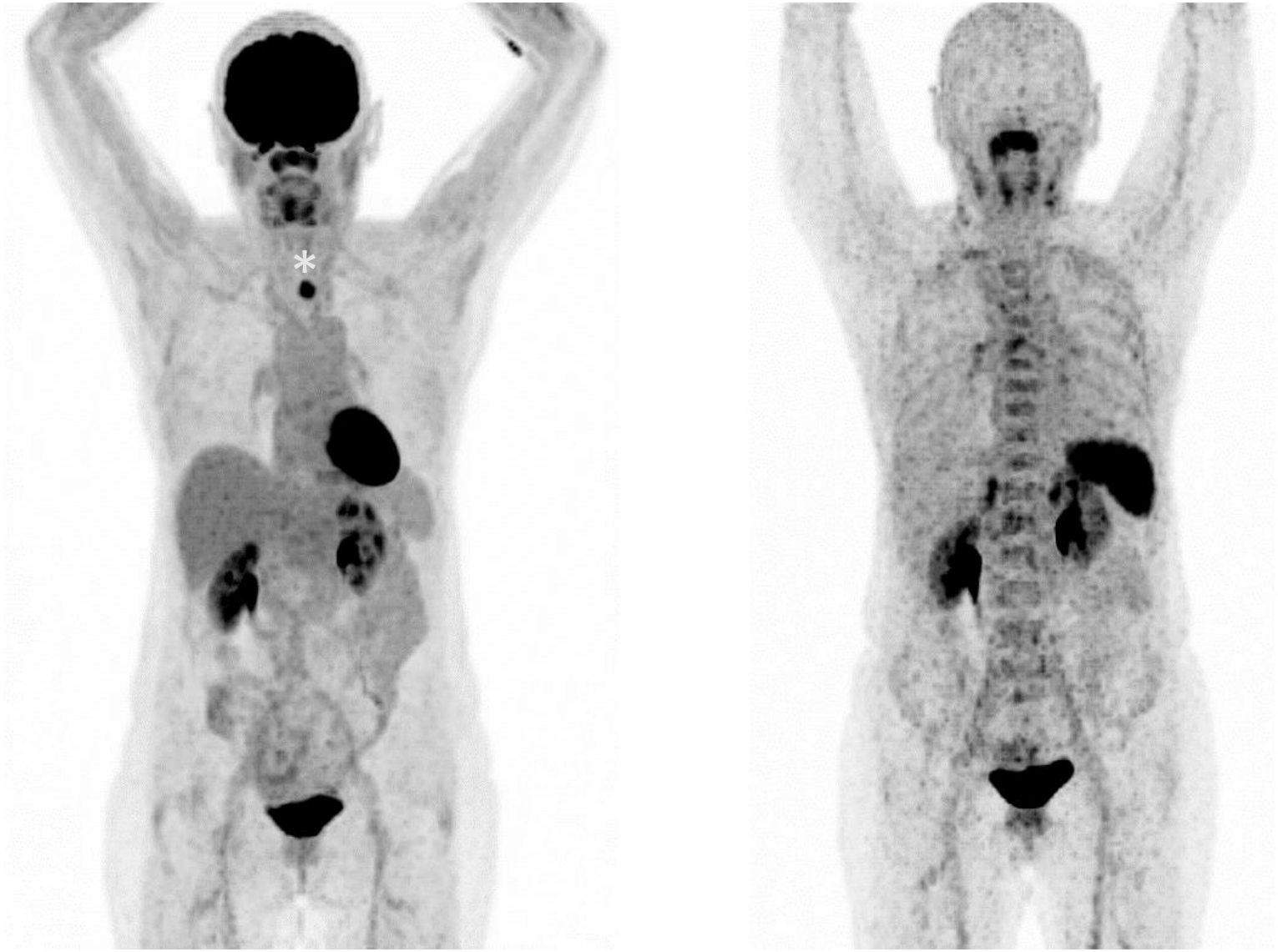

* Focal FDG-uptake was traceable to a thyroid nodule

Supplemental Figure 7: MIPs of FDG/CXCR4 PETs of patient #7

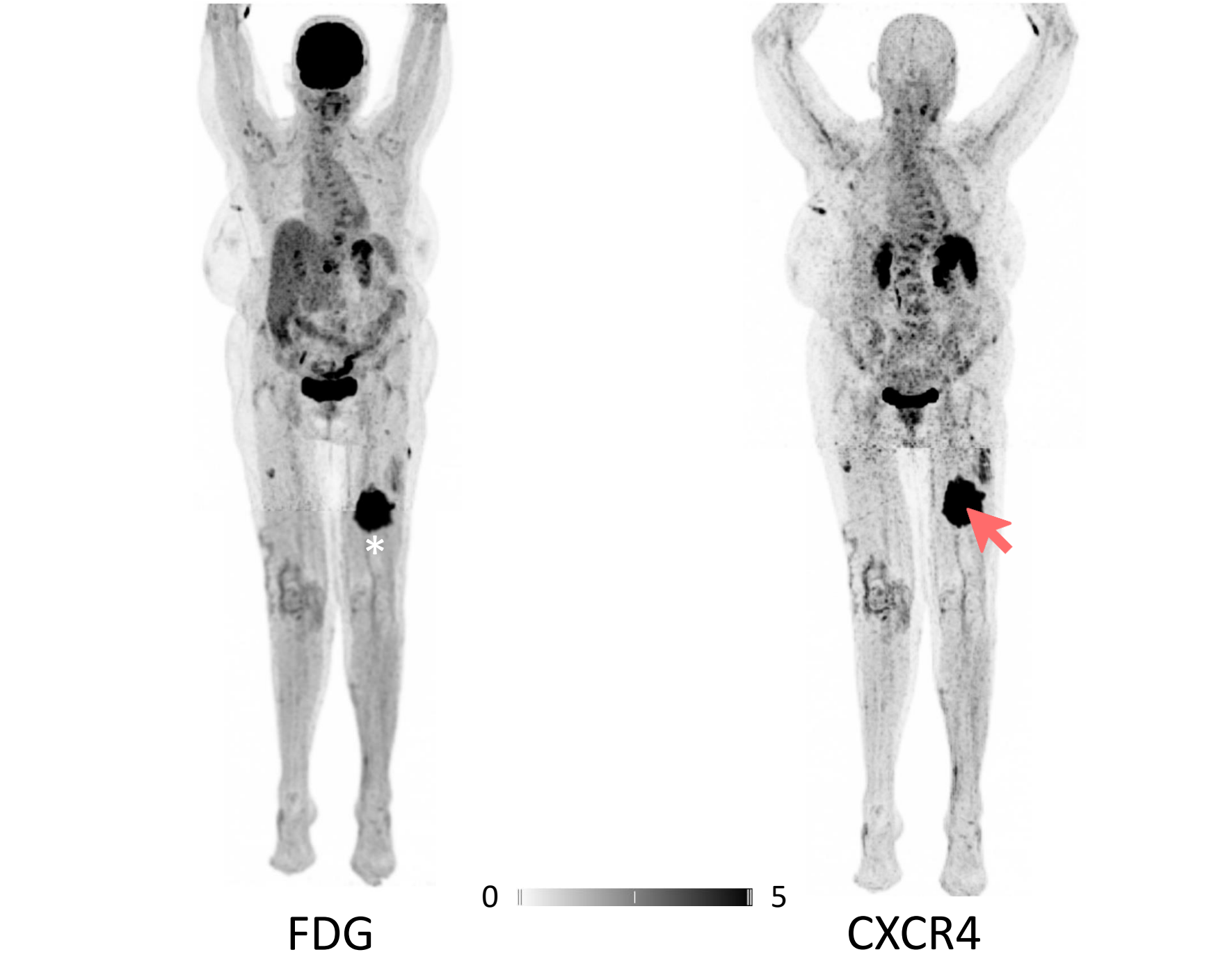

* Lesion was detected by both tracers (CXCR4^{+} / FDG^{+})

Supplemental Figure 8: MIPs of FDG/CXCR4 PETs of patient #8

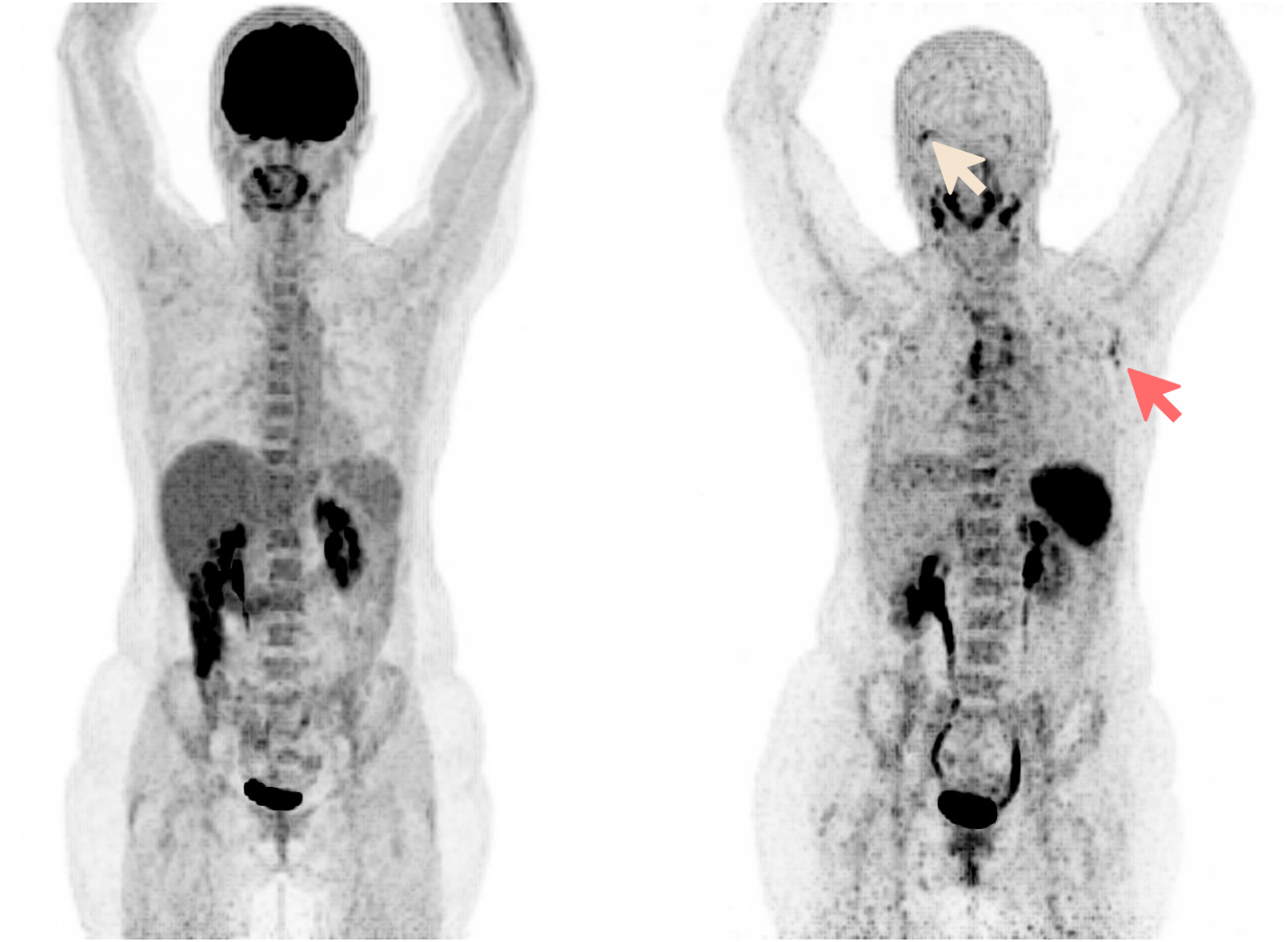

Biopsy of the right conjunctiva (beige arrow) could not confirm MZL

Supplemental Figure 9: MIPs of FDG/CXCR4 PETs of patient #9

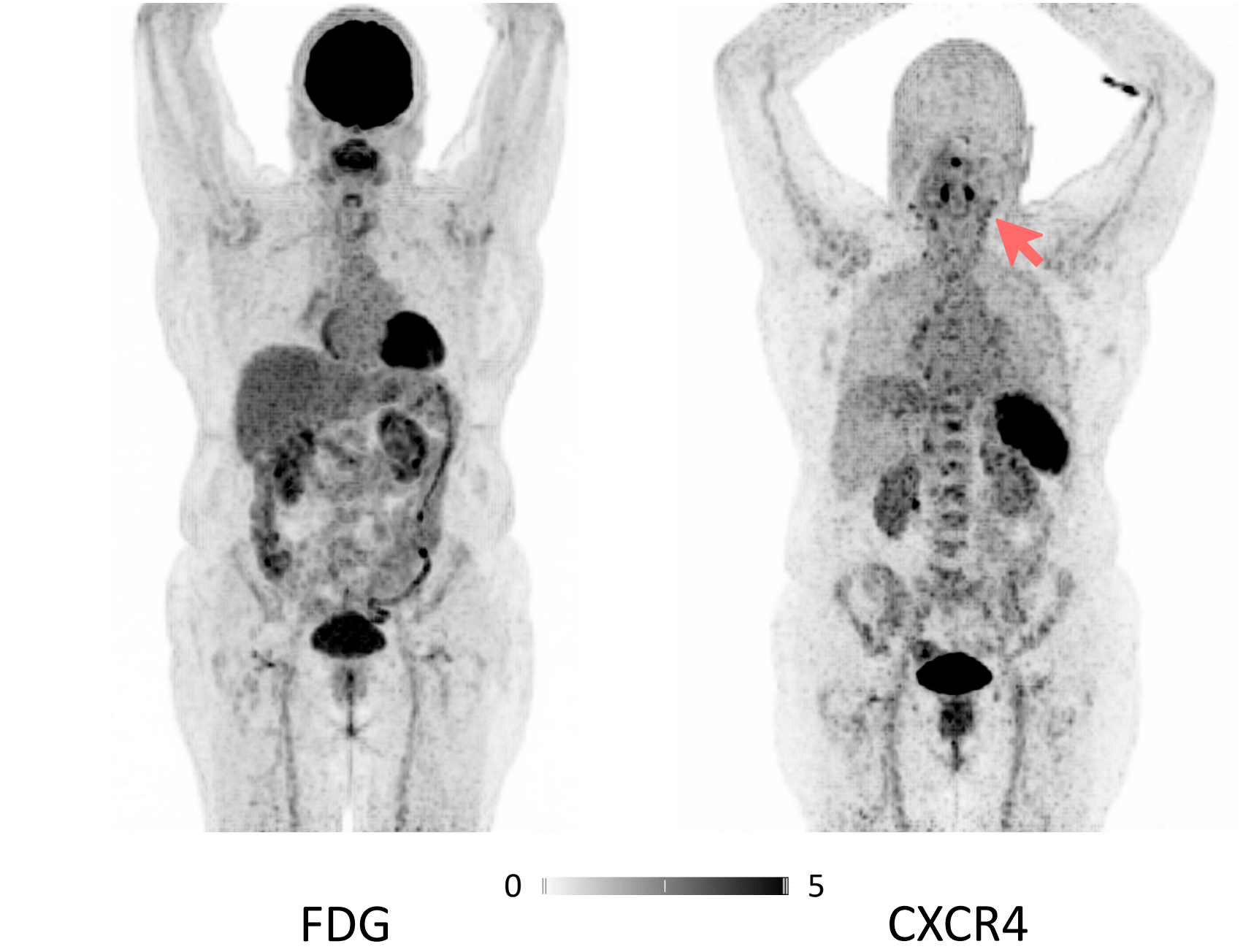

Supplemental Figure 10: MIPs of FDG/CXCR4 PETs of patient #10

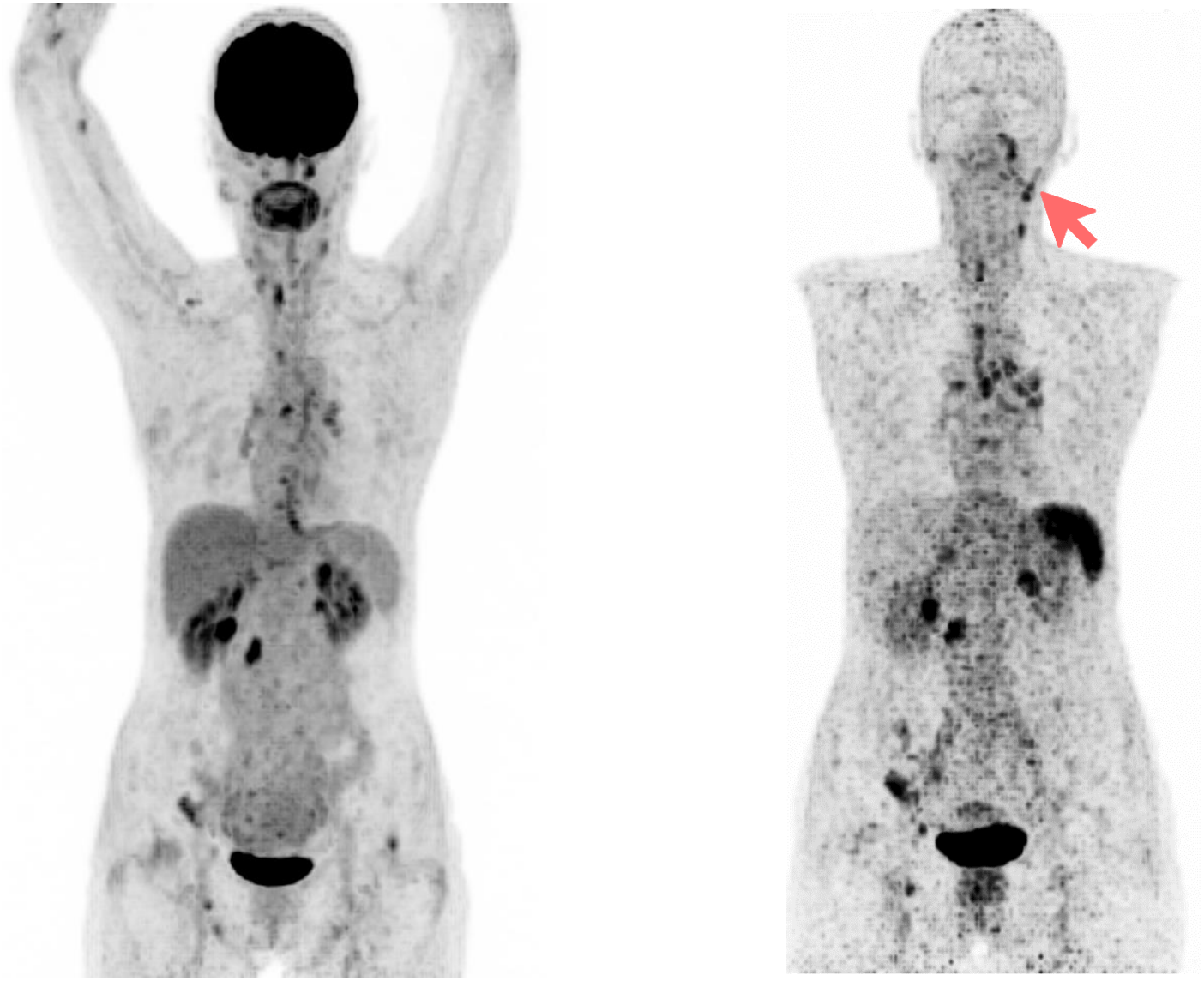

Supplemental Figure 11: MIPs of FDG/CXCR4 PETs of patient #11

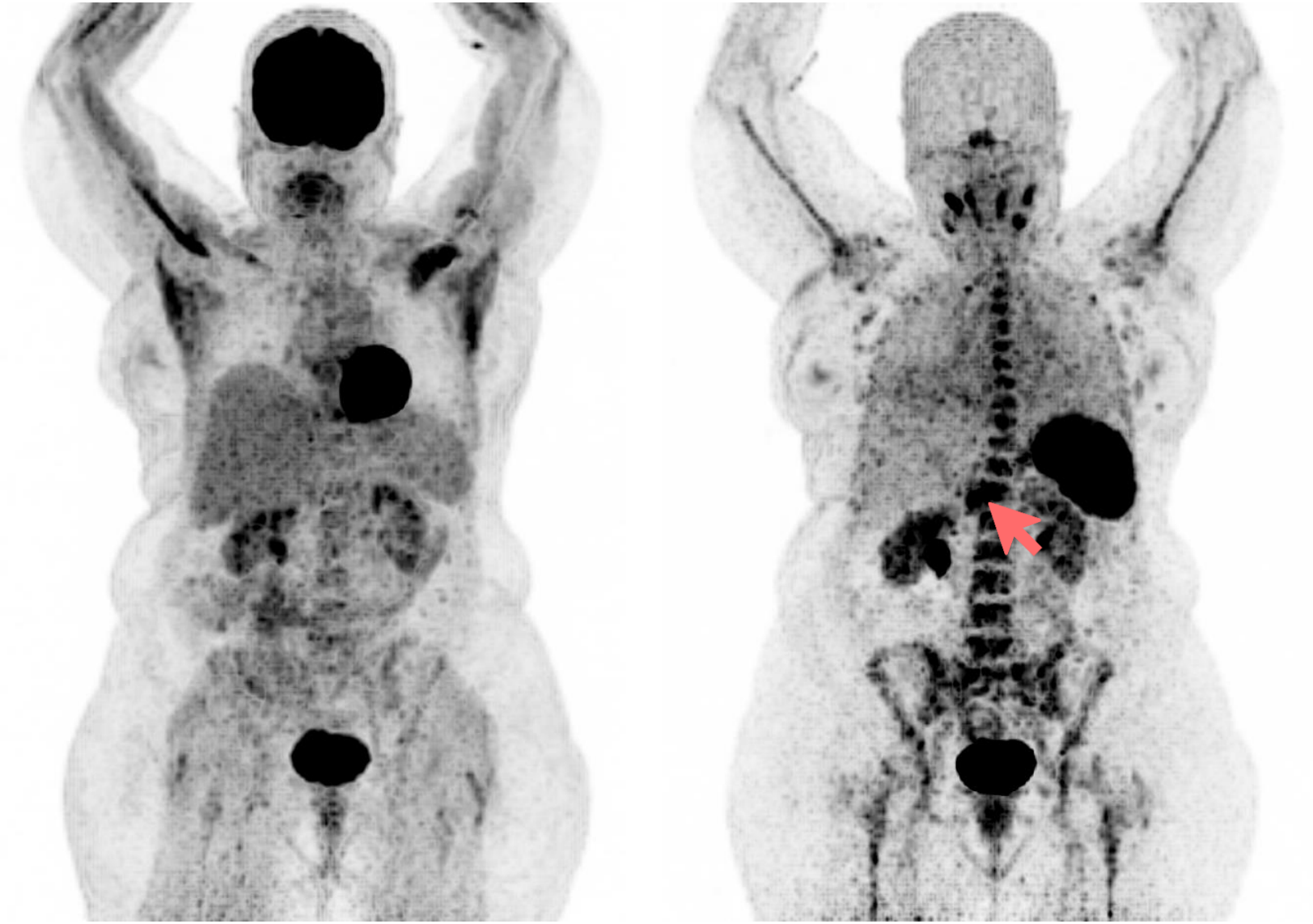

Supplemental Figure 12: MIPs of FDG/CXCR4 PETs of patient #12

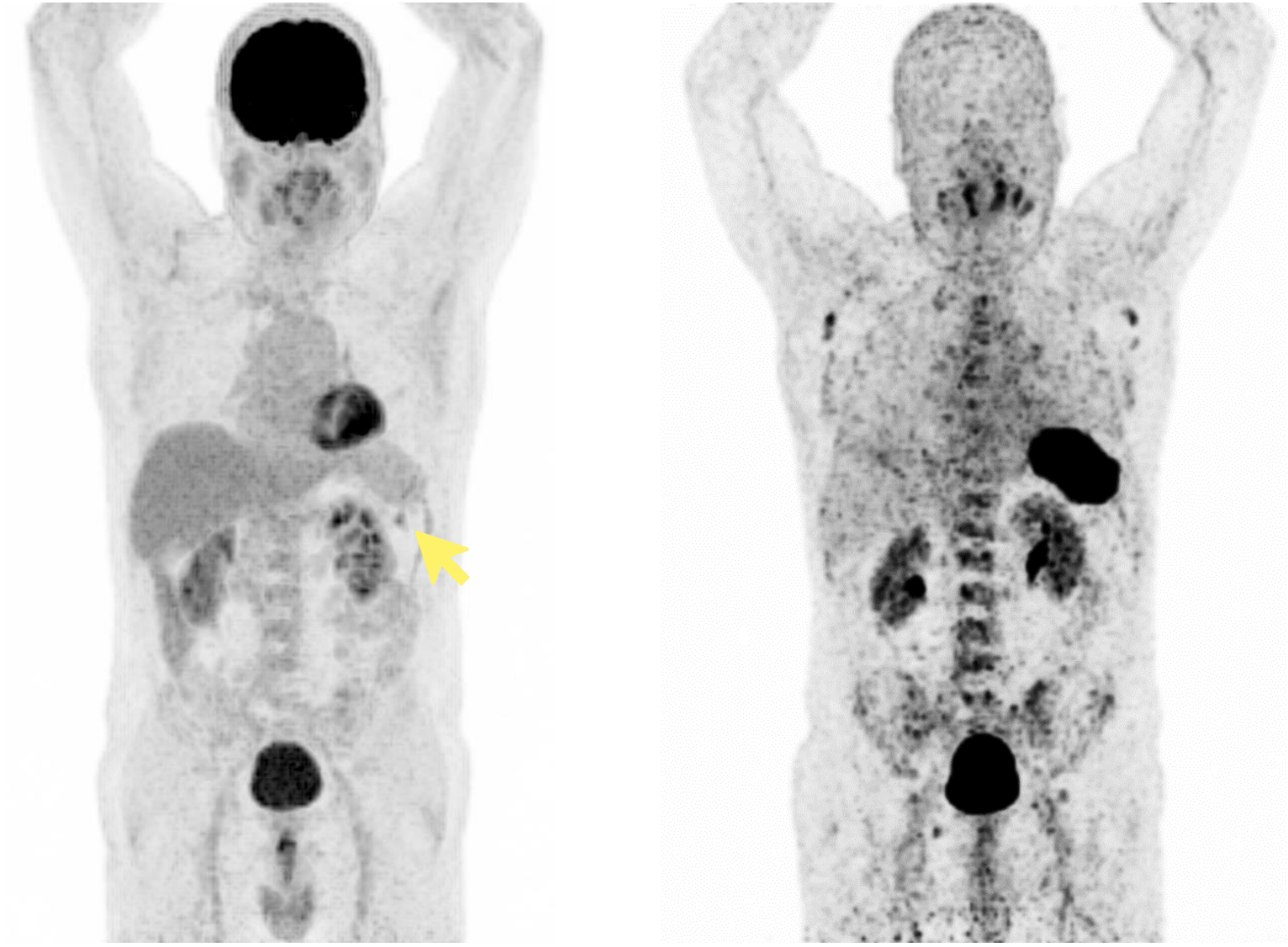

Supplemental Figure 13: MIPs of FDG/CXCR4 PETs of patient #13

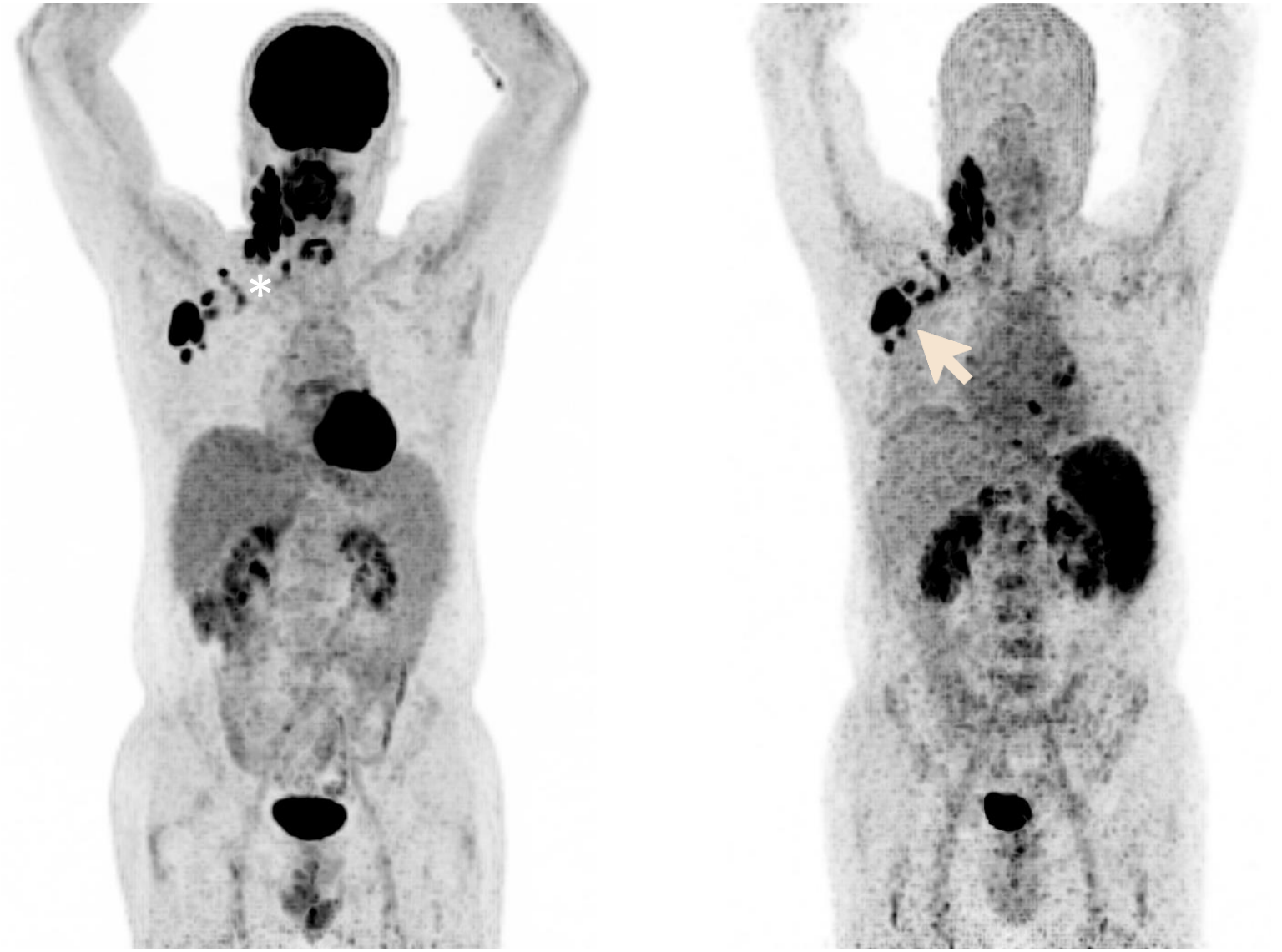

Biopsy of axillary lymph nodes (beige arrow) did not provide sufficient material to confirm MZL;
* lesions were detected by both tracers ($CXCR4^+$ / FDG^+)

Supplemental Figure 14: MIPs of FDG/CXCR4 PETs of patient #14

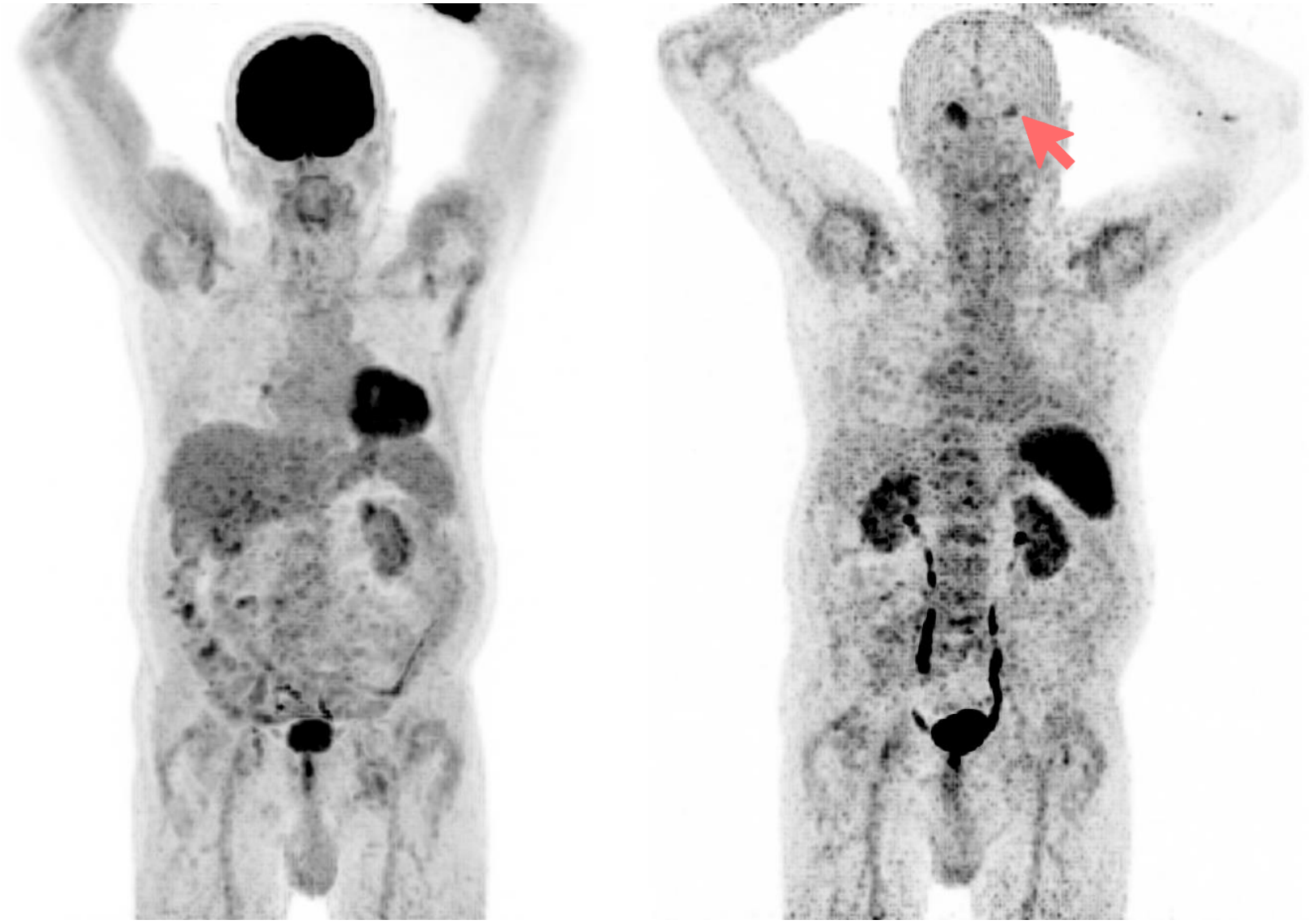

Supplemental Figure 15: MIPs of FDG/CXCR4 PETs of patient #15

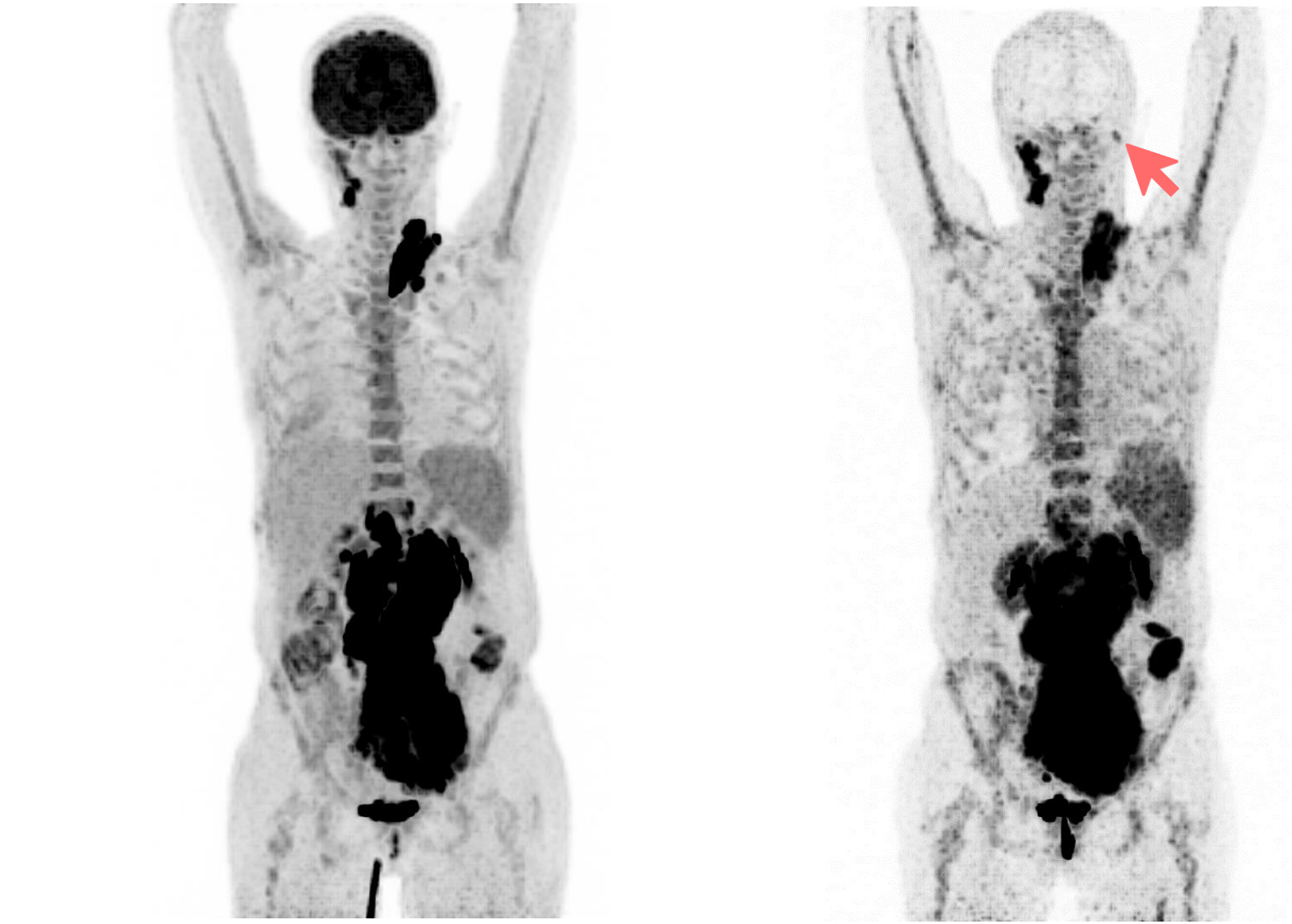

Supplemental Figure 16: MIPs of FDG/CXCR4 PETs of patient #16

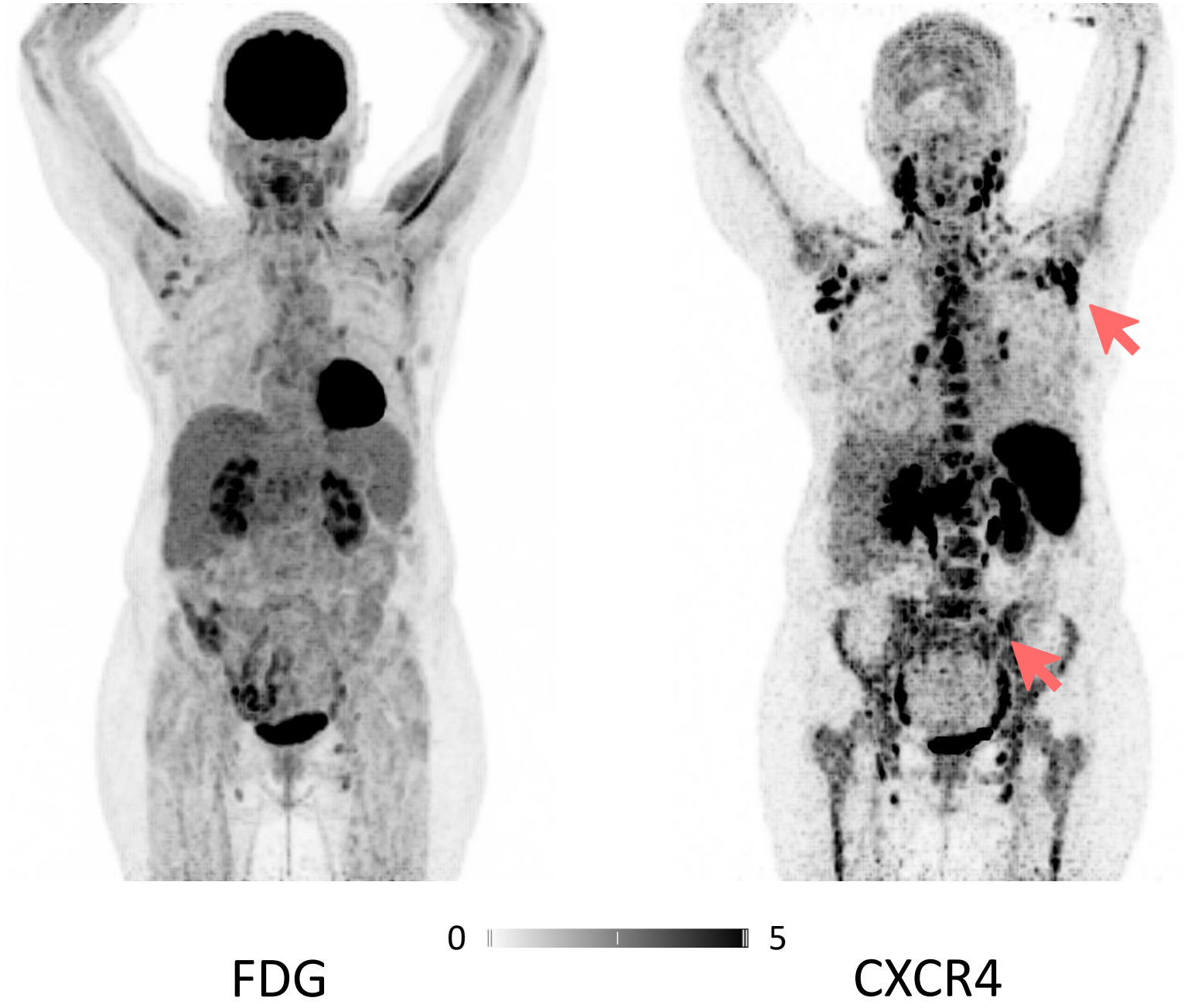

Supplemental Figure 17: MIPs of FDG/CXCR4 PETs of patient #17

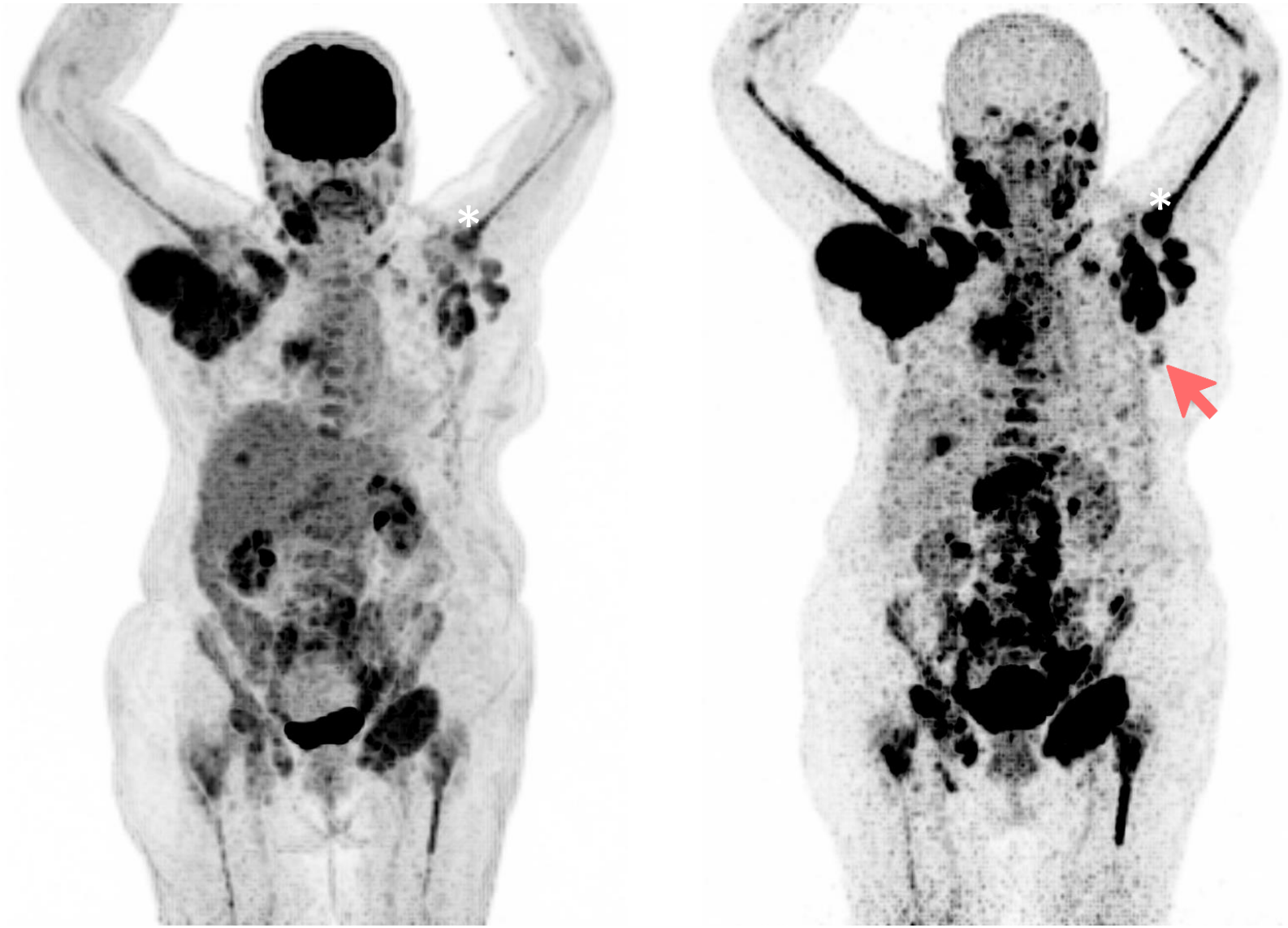

* Although imaging results strongly suggest a bone marrow infiltration, no histologic proof could be obtained

Supplemental Figure 18: MIPs of FDG/CXCR4 PETs of patient #18

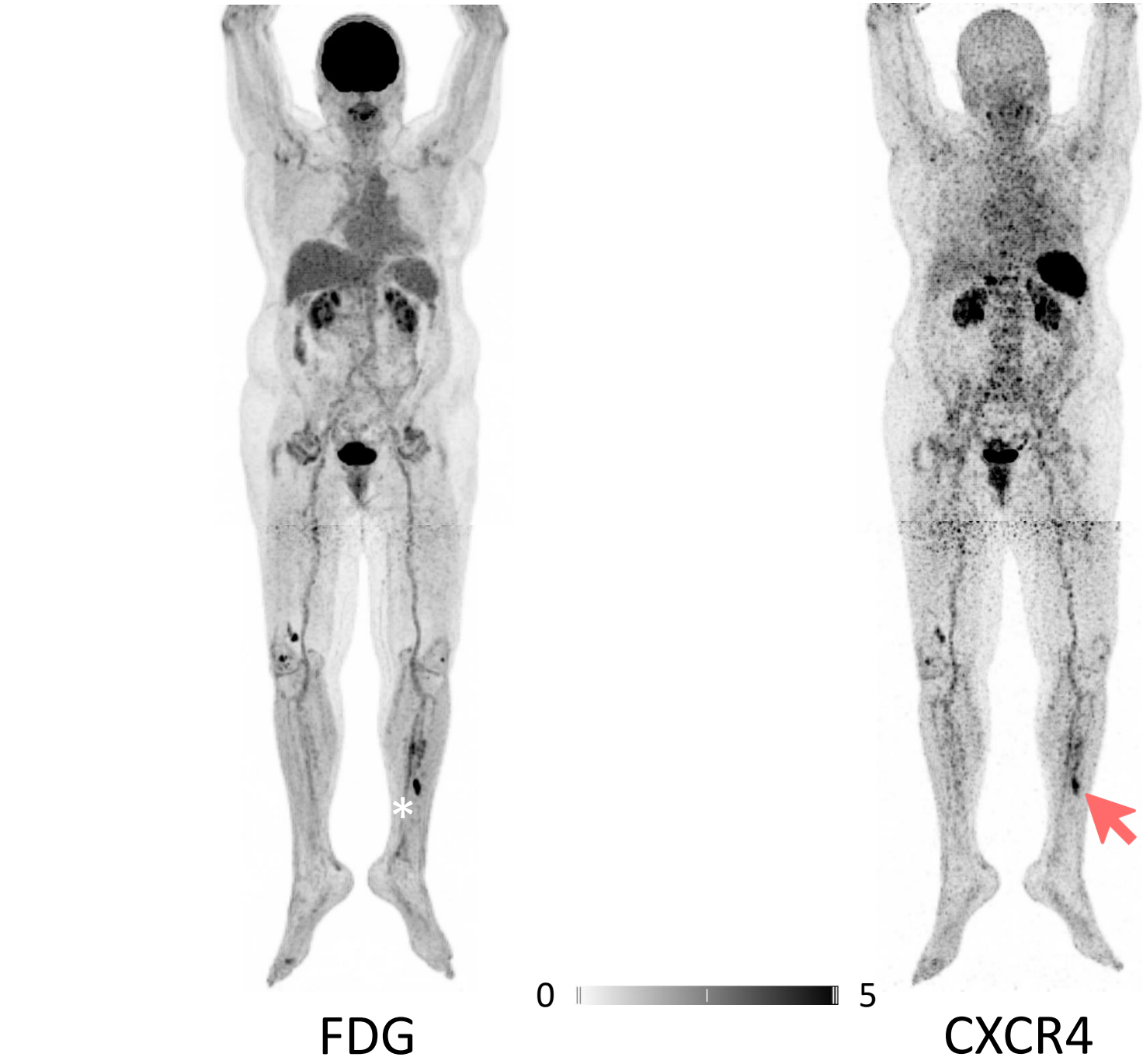

* Lesions were detected by both tracers (CXCR4^{+} / FDG^{+})

Supplemental Figure 19: MIPs of FDG/CXCR4 PETs of patient #19

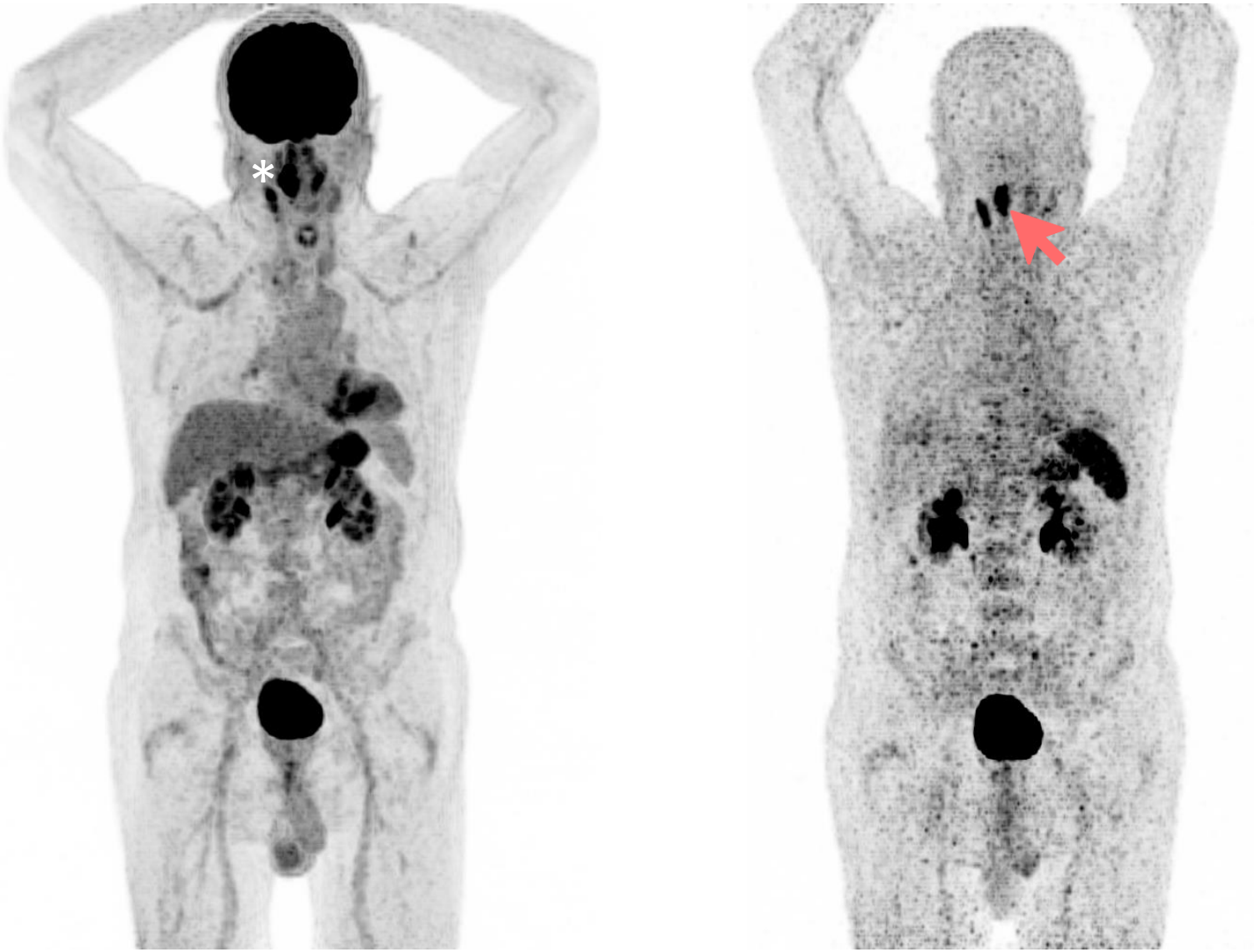

* Lesions were detected by both tracers (CXCR4^{+} / FDG^{+})

Supplemental Figure 20: MIPs of FDG/CXCR4 PETs of patient #20

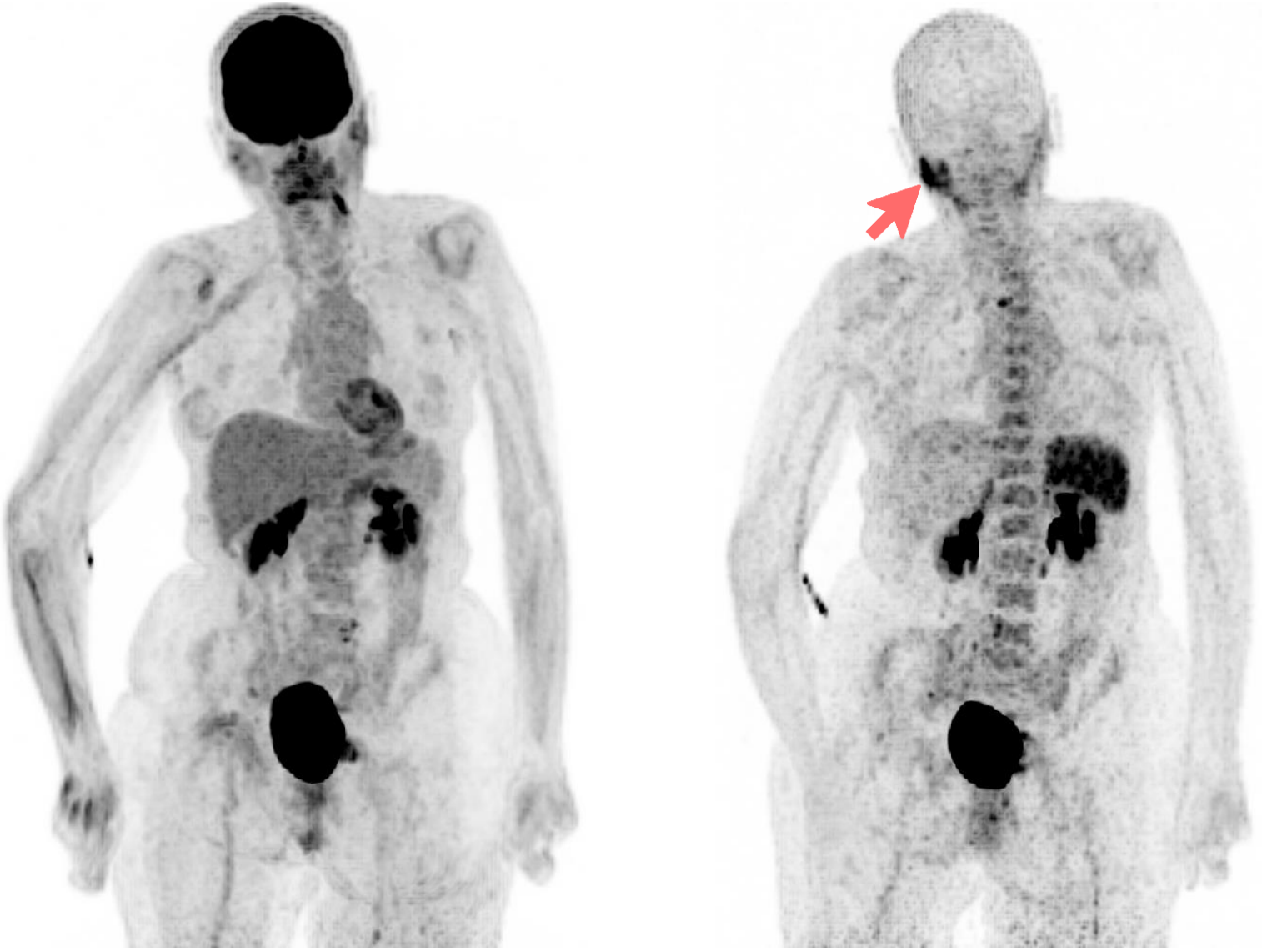

Supplemental Figure 21: MIPs of FDG/CXCR4 PETs of patient #21

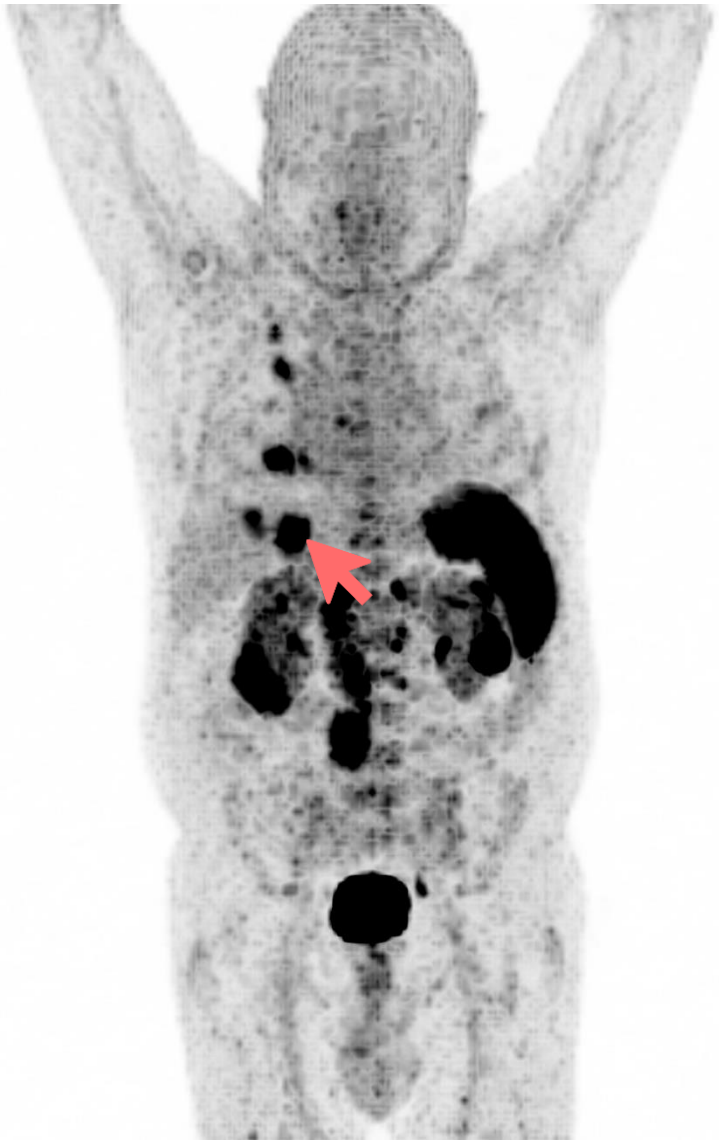

0 5

FDG

CXCR4

Supplemental Figure 22: MIPs of FDG/CXCR4 PETs of patient #22

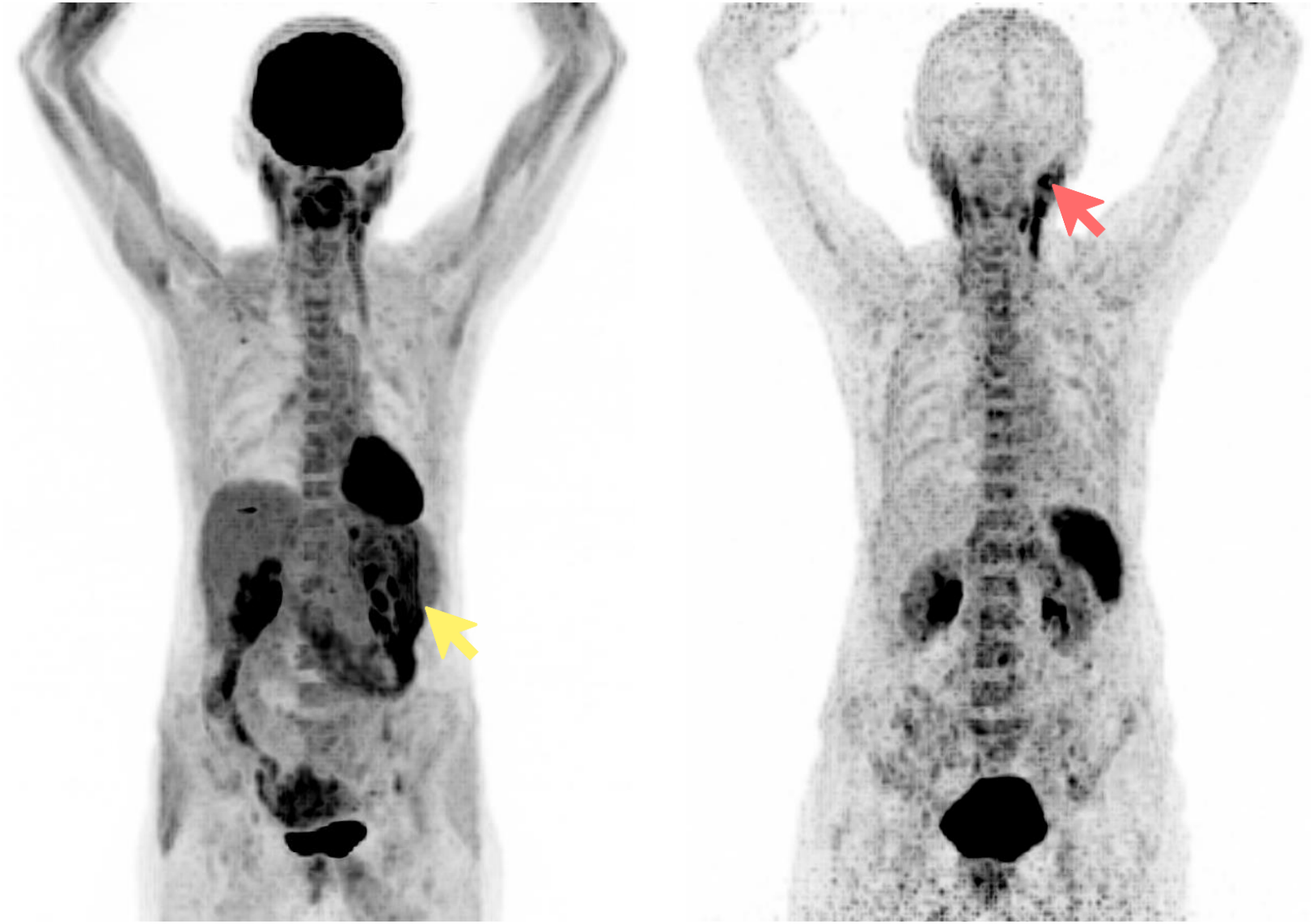

Endoscopy and tissue biopsy revealed florid gastritis in this CXCR4^{-} / FDG^{+} lesion (yellow arrow)